Effect of Gemini Surfactants on Amyloid Beta Aggregation

by

Mehrnoosh Bahmani

A thesis
presented to the University of Waterloo
in fulfillment of the
thesis requirement for the degree of
Master of Science
in
Pharmacy

Waterloo, Ontario, Canada, 2013

AUTHOR'S DECLARATION

I hereby declare that I am the sole author of this thesis. This is a true copy of the thesis, including any required final revisions, as accepted by my examiners.

I understand that my thesis may be made electronically available to the public.

Abstract

Alzheimer's disease (AD) is a progressive dementia affecting cognition, behavior, and functional status and there is no cure which exists for it. In AD, Amyloid Beta (Aβ) peptides form aggregates that are neurotoxic in the brain. Hence, molecules that are able to prevent Aß aggregation could be effective in AD treatment. Gemini surfactant (GS) molecules consist of two hydrophilic heads separated by a covalently bound spacer and two hydrophobic tails. Their structure gives rise to a number of unique properties, including low critical micelle concentrations, the ability to form multiple types of aggregates (governed primarily by the nature of the spacer group) and enhanced ability to bind to polymers. These properties make gemini surfactant a good choice for solubilizing very hydrophobic materials such as Aß. The aim of this study was to examine various GS structures to help us to understand their interaction with Aβ and the influence of spacer group in Aβ disassembly.

We employed 12-carbon tail GS with varying spacer groups of different hydrophilicities, such as: $(-CH_2-CH_2-O)_m$, $(-CH_2)_m$, $N(CH_2)_m$, $OH(CH_2)_4$ and $(OH)_2(CH_2)_4$. Surface tension measurement, isothermal titration calorimetry (ITC) and dynamic light scattering (DLS) have been employed to observe the gemini-Aβ interaction.

Surface tension measurements did not show a typical surfactant-polymer interaction; rather, the presence of Aß induced aggregate formation at concentrations well below the cmc. Headgroup areas were observed to decrease for some of the surfactants in the presence of Aß, which may result from partial neutralization of the surfactant headgroups and a relaxation of electrostatic repulsion resulting in decreased head group areas. ITC results suggest substantial

reorganization of Aß/gemini surfactant aggregates, with distinct difference seen depending upon the nature of the headgroup. It was observed that in $12\text{-}(CH_2)_n\text{-}12$ (n=2,3,4,7) shorter spacer gemini surfactants have stronger interaction with Aß than the ones with longer spacers. In the $12\text{-}4(OH)_n\text{-}12$ series, a stronger interaction was observed in the GS with 2 hydroxyl groups compared to one hydroxyl group GS. For $12\text{-}(EO)_n\text{-}12$ GS, a stronger interaction was observed in that GS with two ethoxy groups. In the 12-XN-12 series, although the 8N spacer is more hydrophilic than 5N, the interaction of 12-5N-12 with Aß was stronger than that of 12-8N-12. The particle size data also revealed that there is an interaction between gemini surfactant and Aß. It appeared that mixed micelles formed when the surfactant concentration increased in the Aß solution. Overall, it was observed that changes in the length and hydrophilic character of the gemini surfactant spacer influenced the type of interaction and gemini-Aβ conformation.

Acknowledgements

I would like to express my sincere gratitude to my supervisor, Prof. Shawn Wettig, for his patience, motivation, enthusiasm, and immense knowledge. His guidance helped me in all the time of research and writing of this thesis.

Thanks to Prof. Roderick Slavcev, Prof. Michael Beazely and Prof. Jonathan Blay for their valuable comments and careful reading of the draft.

I would like to thank my friends in the school of pharmacy specially Lizzie Wang, Amany Kamel, and Samantha Shortall for their generous support.

Last but not the least, I would like to thank my family for all their love and encouragement.

Dedication

I lovingly dedicate this thesis to my husband, Mehdi.

Table of Contents

List of Figures

List of Tables

List of Abbreviations

a_0	head group areas
Aß	Amyloid Beta
AChEI	Acetylcholinesterase Inhibitors
ACE	Angiotension Converting Enzyme
AD	Alzheimer's Disease
AFM	Atomic Force Microscopy
AICD	APP intracellular domain
APP	Amyloid Precursor Protein
BACE1	Beta Amyloid Precursor Protein-Cleaving Enzyme 1
BBB	Blood–Brain Barrier
CAC	Critical Aggregation Concentration
CMC	Critical Micelle Concentration
CTF99	C-terminal fragment
DTAB	dodecyl trimethyl ammonium bromide
ECE	Endothelin converting enzyme
EM	Electron microscope
GS	Gemini surfactants
HFIP	Hexafluoroisopropanal
HMP	Hexadecyl-N-methylpiperidinium
IDE	Insulin Degrading Enzyme
ITC	Isothermal titration calorimetry
Lenti-Nep	lentiviral vector expressing human neprilysin
LRP-1	lipoprotein receptor related protein
NEP	Neprilysin
NFTs	Neuritic plaques and neurofibrillary tangles
NNLS	non-negative least squares
NSAIDs	Non-Steroidal Anti-Inflammatory Drugs
PPAR γ	peroxisome proliferator activated receptor-γ
R	Gas constant
RAGE	receptor for advanced glycation end products

X_{cmc}	surfactant mole fraction at cmc
ΔG°_{mic}	free energy of micellization
ΔG	Gibbs free energy per mole of surfactant aggregation to a polymer
ΔG°_{PS}	Gibbs free energy per mole of surfactant involved in polymer/surfactant interaction
sAPPß	N-terminal fragment
SDS	sodium dodecyl sulfate
T	absolute temperature
ΔS	entropy
Γ	Gibbs surface excess concentration for the surfactant at the air water interface

Chapter 1: Introduction

1.1 Introduction and Review of Prior Knowledge about Alzheimer's disease (AD)

Alzheimer's disease (AD) is the most prevalent type of dementia affecting cognition, behavior, and functional status (1). The clinical presentations of Alzheimer's disease are: 1) memory loss (2), 2) gradual cognitive decline (3), 3) behavioral and psychological disturbances at moderate (4), 4) frequent loss of daily function (5-8). According to a census in 2009 (9) the number of people suffering from dementia in the world is about 35.6 million and this number is predicted to increase to 115.4 million by the year 2050. AD is the fifth cause of death in United States for people above age 65 and is the main cause of dementia in late-life dysfunction. Approximately 5.3 million Americans have AD; this number is predicted to increase to 13.2 million by the year 2050 (7). There is currently no cure and the pathophysiologic mechanisms leading to Alzheimer's disease are not completely known (7).

1.2 Pathophysiology of AD

1.2.1 Cholinergic hypothesis of AD

In the early 1970s, the pathology of AD was explained as a neurochemical abnormality. Different studies with brains of AD patients have shown the relationship between acetylcholine and memory and confirmed that there is a reduction in choline uptake and acetylcholine (ACh)

1

release. These findings have led to the cholinergic-deficit hypothesis (10,11). Blocking the central cholinergic activity resulted in memory impairment, whereas using cholinergic agonists reversed the effect (12,13). The acetylcholine receptors are integral membrane proteins to which acetylcholine binds. These receptors consist of nicotinic and muscarinic receptors (14). Various studies have observed a correlation between declining acetylcholine receptors in the brain and AD (15,16). Activation of acetylcholine receptors leads to the elevation of the cytoplasmic calcium level that mediates calcium-dependent intracellular processes responsible for learning and memory (17). The lack of cholinergic function is related to cognitive dysfunction. Therapeutic interventions for treatment of cholinergic dysfunctions include cholinesterase inhibition, choline precursors, postsynaptic cholinergic (18) stimulation and presynaptic cholinergic stimulation. These strategies are not effective in treating AD since they cannot prevent neuronal degeneration; however, they can stabilize cognitive decline for about 6 months (19,20,21).

1.2.2 Neurofibrillary Tangles

Two pathophysiological hallmarks of Alzheimer's disease are senile plaques (consisting of amyloid ß peptide) and neurofibrillary tangles (22). Neurofibrillary tangles are comprised mainly of the hyperphosphorylated tau protein (23) which, in normal neurons, is involved in the assembly and stability of microtubules as well as in axonal transport (24,25). Destabilization of microtubules, which form the neuronal cytoskeleton, can be an important factor in the pathogenesis of AD (26) (Figure 1.2.2.1). Protein kinases and protein phosphatases are

responsible for phosphorylation and dephosphorylation of tau protein, respectively (27). The

consequence of imbalance in the enzyme activities is hyperphosphorylation and neurofibrillary

tangle formation which cause neuronal cell death (11,28,29).
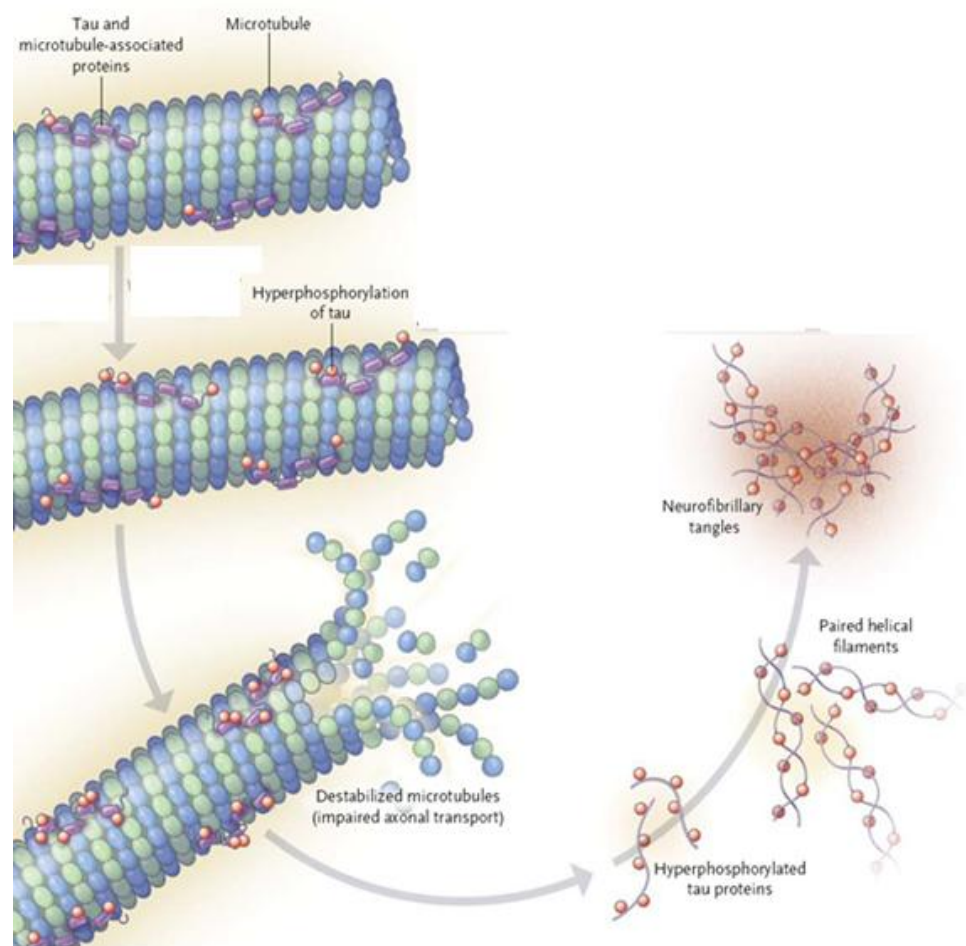
Figure 1.2.2.1: Tau binding to the microtubules. Tau binding promotes microtubule assembly
and stability. Excessive kinase, reduced phosphatase activities, or both, cause
 hyperphosphorylated tau to detach and self-aggregate, and microtubules to destabilize. Adapted
from (30).

1.2.3 Amyloid Beta Peptide (Aβ) formation

In healthy people, the rate of Aβ production equals the clearance rate; whereas in Alzheimer patients the Aß production rate is significantly greater than the clearance rate. It has been shown that in the brain of AD patients, there are amyloid plaques that consist of Aβ fibrils. In fact, Aβ protein aggregates as toxic oligomers that induce local inflammation, neurotoxicity, and cell death (11).

Aβ is a peptide consisting of 36 to 43 amino acids (Figure 1.2.3.1). It is synthesized from amyloid precursor protein (APP) by the action of beta amyloid precursor protein-cleaving enzyme 1(BACE1), α secretase and γ-secretase. According to the amino acid sequence of Aβ (Figure 1.2.3.1), 25 hydrophobic amino acids in Aβ form a hydrophobic core. Previous research indicates that the region between amino acid 17 and 21 of Aβ has high hydrophobicity. The probability of ß sheet formation is high in residues 6 and 8 as well as residues 23 and 27. The residues 34-42 are very hydrophobic and highly insoluble, and have been implicated in nucleating amyloid fibril formation (31).

APP is a glycosylated transmembrane protein, consisting 695 of amino acids, that has extracellular and intracellular domains. Three proteinase enzymes named α, ß and γ secretase can cut APP at specific sites. α secretase cleaves APP and generates neuroprotective sAPPα. ß secretase is responsible for the amyloidogenic process, BACE1 cuts the APP to the N-terminal fragment (sAPPß) and a C-terminal fragment (CTF99) that has 99 amino acids in its structure. Then a second BACE1 cleavage site in APP is cut by BACE1 and yield CTF89. Subsequently,

4

the γ secretase complex cleaves the CTF89 and yields Aß and APP intracellular domain (AICD) (Figure 1.2.3.2) (32).

Aβ42 Aspartic acid[1]- **Alanine[2]**- Glutamic acid[3]- **Phenylalanine[4]**- Arginine[5]- Histidine[6]- Aspartic acid[7]- Serine[8]- **Glycine[9]**- Tyrosine[10]- Glutamic acid[11]- **Valine[12]**- Histidine[13]- Histidine[14]- Glutamine[15]- Lysine[16]-**Leucine[17]**- **Valine[18]**- **Phenylalanine[19]**- **Phenylalanine[20]**-Alanine[21]- Glutamic acid[22]- Aspartic acid[23]- **Valine[24]**- **Glycine[25]**- Serine[26]- Asparagine[27]- Lysine[28]- **Glycine[29]-alanine[30]**- **Isoleucine[31]**- **Isoleucine[32]**- **Glycine[33]** **Leucine[34]**- **Methionine[35]**- **Valine[36]**- **Glycine[37]**- **Glycine[38]**- **Valine[39]**- **Valine[40]**- **Isoleucine[41]**- **Alanine[42]**-

---

Figure 1.2.3. 1: The amino acids in AB(1-42). The amino acids in bold are hydrophobic (33).
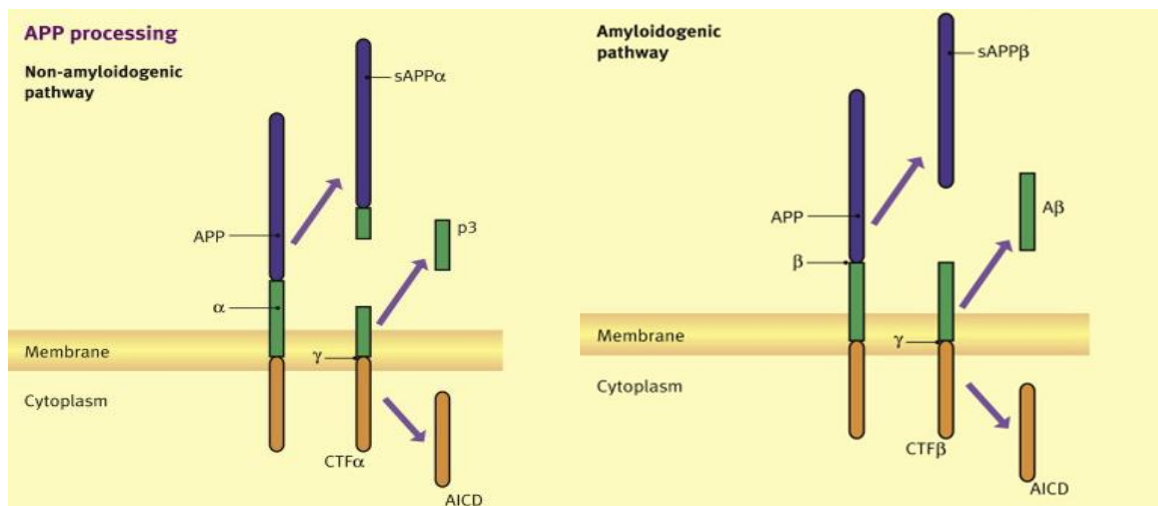
Figure 1.2.3. 2: *In vivo* **synthesis of Aß.** The APP is metabolized throughout the non-amyloidogenic pathway. The action of α and ß secretases is producing sAPP α and AICD. In The amyloidogenic pathway ß secretase is involved in releasing sAPP ß and then γ-secretase responsible for the production of AICD and Aß. Adapted from (34).

1.2.4 Aß assembly

Two stages of Aβ fibrillogenesis are nucleation and fiber formation. Aß monomers first produce micelles, and then the micelles turn into an ordered nucleus that has specific sites for the addition of monomers. The formation of Aß protofibrils is the consequence of adding more monomers to the nucleus, and then these protofibrils turn into mature fibrils (Figure 1.2.4.1) (35). Also, there is equilibrium between particles in part A and B (Figure 1.2.4.1). When the peptide concentration reaches the critical point, micelles form. The transition of part A to part B includes two processes, new fibril formation and elongation of existence fibrils. In fact, nucleus can grow by the addition of dimers, monomers or micelles (36).
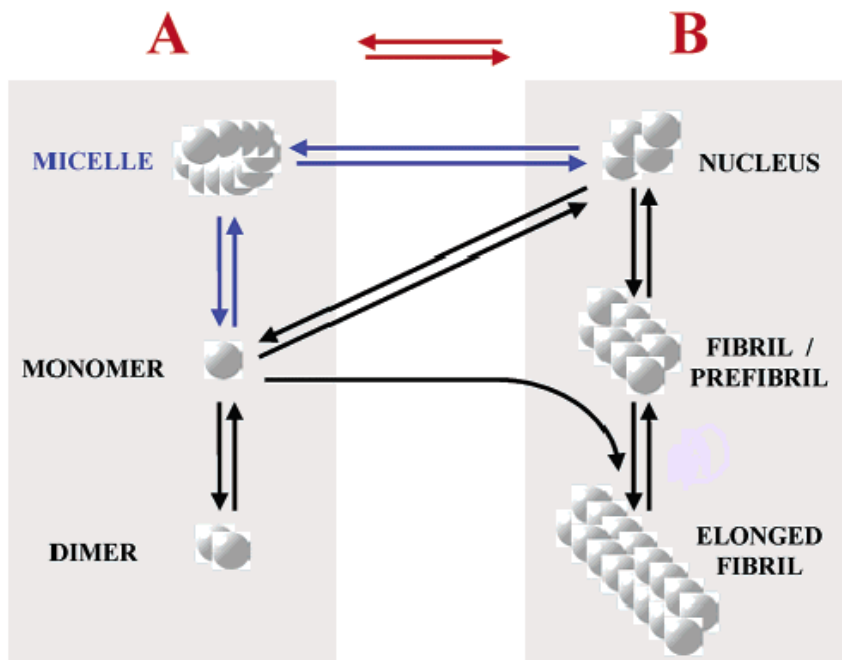
Figure 1.2.4.1. Aβ aggregation. Native Aß turns to fibril through fibrillogenesis process. Adapted from (36)

1.2.5 Anti amyloid therapy

Aß fibril plays an important role in AD pathophysiology. The relationship between Aß fibril and AD is called amyloid hypothesis (37). According to this hypothesis the consequences of Aß fibrils accumulation in the brain are oxidative stress, neuronal destruction, synaptic dysfunction and appearance of signs and symptoms of AD. Formation of amyloid oligomers causes local inflammation and neurotoxicity in the brain. Aß formation leads to the tau protein folding in the neuronal cells and cell death. Neuronal cell death leads to neurotransmitter imbalance in the brain and cognitive deficiencies in AD. According to the above pathways leading to AD, there are three strategies which can be used in AD treatment (Figure 1.2.5) (11).
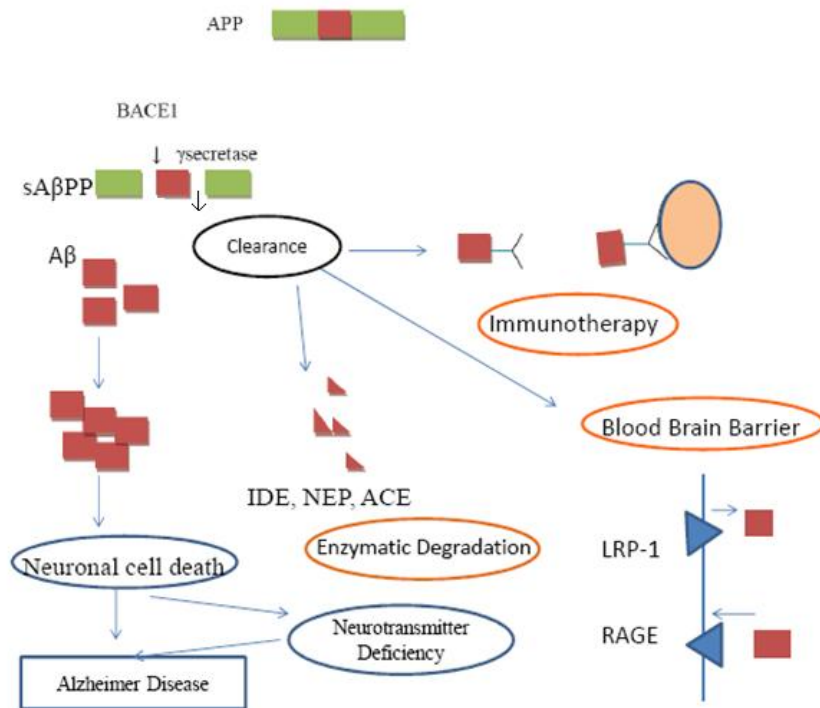
Figure 1.2.5.1 The amyloid cascade and the potential therapeutic interventions. Pharmacotherapy for AD can be aimed at decreasing Aß generation, stimulating Aß clearance or preventing aggregation of Aß. Adapted from (11).

1.2.5.1 Decreasing Aß production

As Aß is the product of APP cleavage by ß and γ secretase, one strategy in AD treatment can be the inhibition of the enzyme activity (Figure 1.2.5). BACE1 mRNA increases by proinflammatory mediators. Therefore, non-steroidal anti-inflammatory drugs (NSAID) have been suggested to be effective in BACE1 inhibition; due to their ability to control the production of the nuclear transcriptional regulator peroxisome proliferator activated receptor-γ (PPAR γ). The presence of PPAR γ leads to the deactivation of the BACE1 gene promoter and decreases ß secretase mRNA levels. However, experimental data in this area is inconclusive (38).

Prevention of γ secretase activity can also be used to inhibit Aß production. According to a 6 week trial in AD patients, the γ secretase inhibitor LY450139, showed reduction in Aß-40 level in serum.(39). As γ secretase has various substrates, inhibition of this enzyme leads to some adverse effects such as gastrointestinal problems and neurodegeneration (11).

Increasing α secretase activity can be helpful in prevention of Aß production as well as the generation of neuroprotective substance sAPPα (11). α secretase is a member of the ADAM-10 family of protease. It seems that overexpression of ADAM-10 reduces amyloid plaque formation as well as alleviating synaptic plasticity and deficits in spatial learning in animals. Therefore, α secretase activation can be helpful in improving cognitive status in human. The other way to increase α secretase activity is stimulation of muscarine-1 receptor with M1-agonists (e.g. talsaclidine). These agonists are shown to decrease γ-secretase and BACE1 activity as well (11).

1.2.5.2 Increasing Aß clearance

Clearance of Aß from the brain through immunotherapy and enzymatic degradation is another strategy in AD treatment (Figure 1.2.5). Immunotherapy targeting Aβ has been tried using both active and passive immunization. The first trial was active vaccination using a vaccine that contained full length $Aß_{42}$ peptide. Unfortunately, this vaccine caused severe adverse effect (meningoencephalitis), however long term follow up of the patients who received vaccine showed that there was a reduction in cerebrospinal fluid tau compared to the placebo group(40,41). The second active immunization that has been studied was active" Humoral only" immunization. This vaccine contained small peptide sequences of Aß conjugated to a carrier. The study showed that the antibodies to Aß were produced in 80% of patients who received the vaccine (42). In the studies using passive immunotherapy the humanized Anti Aß monoclonal antibodies were used. Some monoclonal antibodies that have been used were bapineuzumab, gantenerumab and solanezumab (43,44).

The mechanism of clearance of Aß by anit-Aß antibody is still unknown (45). However there are some hypotheses that explain it. It has been shown that a class of anti-Aß binds to Aß aggregates and microglial phagocytotic system clears Aß plaques by phagocytosis of the anti- Aß attached to the Aß plaques (46). The second proposed mechanism is that anti-Aß attaches to soluble Aß in the peripheral circulation and makes a peripheral sink condition, resulting in a decrease in the amount of soluble Aß in the bloodstream which therefore causes an efflux of Aβ from the brain back into the peripheral blood stream (47).

Enzymatic degradation is another strategy to increase Aß clearance. Neprilysin (NEP) is a degrading enzyme that has a catalytic site and can cleave regulatory peptides (with up to 50 amino acids) on the N-terminal side of hydrophobic amino acid residues (48), making Aß a substrate for NEP. It was shown that NEP localizes in the pre and post synaptic area. Hence, different studies were conducted to assess the physiological and pathophysiological importance of NEP in nervous system in animal model. In one study, which assessed the effect of NEP on the amyloidogenesis process, a lentiviral vector expressing human neprilysin (Lenti-Nep) was produced and tested in transgenic models of amyloidosis. In that study, to evaluate the anti-amyloidogenic effects of NEP in vivo, lentiviral virus expression NEP gene was injected into the CNS of transgenic mice which develop high level of amyloid deposition. It was observed that amyloid plaques on the Lenti-NEP injected hemispheres were smaller compared to the contralateral side (49).

1.2.5.3 Influencing blood-brain barrier (BBB) transport

There are two enzymes that are responsible in Aß transportation across the BBB; the receptor for advanced glycation end products (RAGE), and the low density lipoprotein receptor related protein (LRP-1). RAGE transports Aß from the systemic circulation across the BBB. LRP-1 is responsible for transporting Aß out of the brain. In AD, RAGE is upregulated and LRP-1 is downregulated, resulting in increased Aß concentration in the brain. As such, any molecule that affects LRP-1 and RAGE activities (i.e., upregulating LRP-1 and downregulationg RAGE) may be efficient in AD treatment (Figure 1.2.5) (11).

1.3 Polymer-surfactant system

1.3.1 Application of polymer-surfactant system

Polymer and surfactant are commonly found in cosmeceutical products. When these two materials are used together in the same product, the possibility of interaction between their molecules increases. This interaction alters the physicochemical properties of the products. Having knowledge about the physicochemical properties of surfactant-polymer system can be helpful in determining how this system works and also give worthwhile insights to scientists who desire to design the surfactant-polymer mixture with some specific properties (50). Aβ is a biomacromolecule (biopolymer) and its structure and aggregation can be affected by surfactants. Different studies show the effectiveness of surfactant molecules in disaggregation of Aβ aggregates (51,52).

1.3.2 Polymer- Surfactant Interaction

The polymer-surfactant interaction has been investigated in different studies (53,54). There are nine possible interactions according to the charge of the polymer and surfactant molecules:

- positive charged polymer-positive charged surfactant,
- positive charged polymer- negative charged surfactant,
- positive charged polymer- uncharged surfactant,
- negative charged polymer- negative charged surfactant,
- negative charged polymer- positive charged surfactant,

- negative charged polymer- uncharged surfactant,

- uncharged polymer- positive charged surfactant,

- uncharged polymer- negative charged surfactant,

- uncharged polymer- uncharged surfactant

If the two components have the same charge, a strong interaction is unlikely due to repulsive interactions. Also, the interactions between nonionic components are unable cause strong interactions between the surfactant and the polymer. The only strong interactions that exist between polymer and surfactant molecules are those within ionic surfactant-neutral polymer systems or ionic surfactant- opposite charged polymer systems (55).

In polymer- surfactant solution, the surfactant interaction with polymer is controlled by Van de Waals, hydrophobic effect, dipolar, acid-base and electrostatic interactions (56). When a surfactant is added to a solution containing polymer molecules, micellization occurs at lower concentration than the surfactant's "critical micelle concentration" (cmc). Surfactant and polymer molecules begin to form complex aggregate structure that looks like a "string of pearls" at a certain concentration that is called "critical aggregation concentration" (cac) which is lower than cmc. Polymer units make surfactant aggregates more stable. In fact, it is assumed that the polymer molecules act as a seed for surfactant molecules (56). The following equation shows the free energy of micellization of a surfactant:

$$\Delta G^{\circ}_{mic} = RT\ln x_{cmc} \qquad \text{(Equation 1.1)}$$

Where X_{cmc} is the surfactant mole fraction at cmc, ΔG°_{mi} is the free energy of micellization, R is the Gas constant and T is the absolute temperature.

12

However, the polymer-surfactant interaction is more complicated than formation of free surfactant micelles. In polymer-surfactant interaction, the surfactant forms both aggregates and micelles. Assuming that the driving force for surfactant attaching onto polymers is the same as the one in a normal free surfactant micellization process, the free energy per mole of surfactant aggregation to a polymer can be calculated by the following equation:

$$\Delta G^{\circ}_{b} = RT\ln cac \qquad \qquad \text{(Equation 1.2)}$$

Where ΔG is Gibbs free energy per mole of surfactant aggregation to a polymer, R is the gas constant, and T is the absolute temperature.

Now by having equation 1.1 and 1.2, we can calculate the free energy per mole of surfactant involved in polymer-surfactant interaction:

$$\Delta G^{\circ}_{PS} = \Delta G^{\circ}_{b} - \Delta G^{\circ}_{mic} = RT\ln \frac{cac}{cmc}$$

where ΔG°_{PS} is Gibbs free energy per mole of surfactant involved in polymer/surfactant interaction. It is important to note that the ratio $\frac{cac}{cmc}$ should be less than 1 (which means cac should be less than cmc), otherwise if cmc is less than cac, it shows that surfactant molecules have more tendency to make surfactant micelles rather than interacting with polymer molecules (56,57).

Surface tension changes are different in a solution that contains surfactant and a solution that comprises a polymer and surfactant together (Figure 1.3.2.1). In the surfactant plot, there is only one break that represents the cmc. However, in the surfactant-polymer plot, the first break (T_1) represents the onset of aggregate formation on the polymer (cac). T_2 is related to the point at

13

which polymer is saturated with surfactant molecules. In the region between T_1 and T_2, the surfactant molecules attach to the polymer. Therefore, not much change is observed in the surface tension of the surfactant-polymer solution. After polymer saturation with surfactant molecules, addition of more surfactant into the solution causes reduction in the solution's surface tension until it reaches the second break (T_3) which is called the cmc. At this point the surface tension of the surfactant-polymer solution does not change significantly (58).
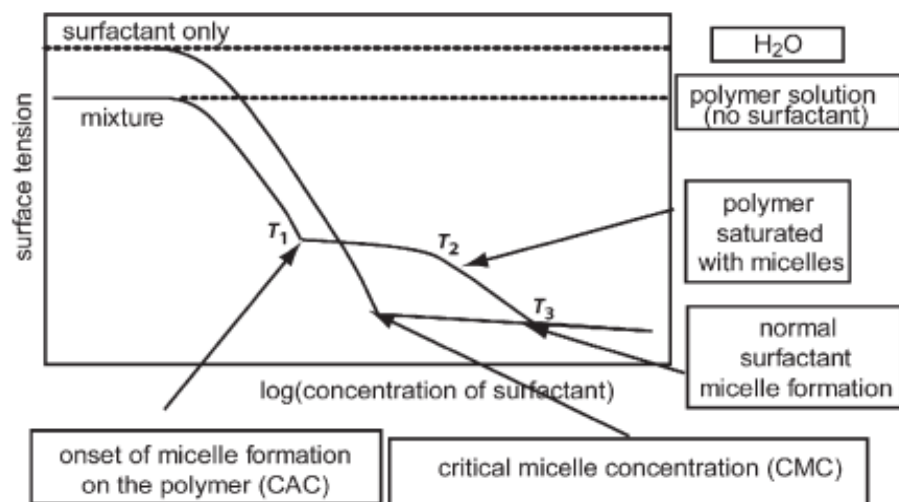
Figure 1.3.2.1: Idealised surface tension of a weakly interacting polymer/surfactant mixture which also interacts at the surface. The surface tension for the surfactant on its own is also shown. Adapted from (58).

1.3.3 Protein-Surfactant Interactions

Proteins are biological heterogeneous polymers which consist of amino acids as their building blocks. Amino acids may have a polar or non polar, ionic, or nonionic side chain. Therefore, proteins can be amphoteric polyelectrolytes or amphiphilic polymers bearing charge

14

density. Structurally speaking, the difference between polymers and proteins is that proteins have less flexibility in their conformation and have much more structural stability than polymers (59).

The interaction between surfactant and protein molecules is divided into two categories: 1- below the cmc 2- above the cmc (60). Below the cmc, protein molecules play an important role in forming micelle-like surfactant clusters. As the surfactant concentration increases, the binding sites in protein become saturated and surfactant molecules tend to become micelles. At this point the protein starts to become unfolded which means the secondary and tertiary structure of a protein will be affected by the addition of surfactant (60).

In protein-surfactant interaction, surfactant causes protein unfolding, refolding (i.e., after the native protein structure is disturbed by surfactant molecules, it can be refolded by the force of surfactant molecules; however, the refolded structure is not the same as the original native conformation), enzyme activation and protein solubilization. In addition, surfactant molecules can affect the protein stability or enzyme activity. The mechanisms that are involved in these interactions are important to analyze and optimize the protein-surfactant interaction (61).

The surfactant can be found in various states in the solution: monomeric, shared micelle and regular micelle. If the surfactant is ionic, its shape and ionic strength make the surfactant-protein interaction more complex. Anionic surfactants attach to the cationic part of the protein and cationic surfactants bind to the anionic region of the protein. The hydrophobic areas in surfactant and protein bind together (60).

There are various ways for denaturing protein molecules, such as heating or adding surfactant in certain concentration. As the surfactant and protein molecules are both amphiphilic,

the possibility of interaction between them is high. The surfactant molecule binds to protein in a stage that the conformation of protein will completely change, and this change is irreversible because the secondary and tertiary structure of protein will be destructed. In fact, if the surfactant molecule is removed from the protein solution, the protein molecule cannot conform to its original structure (59).

1.4 Gemini surfactant

The structure of the gemini surfactant (GS) contains two polar head groups and two non-polar tails, with a spacer covalently linking the two polar groups (Figure 1.4.1). Their structure can be thought of as essentially a dimer of two traditional surfactant molecules. The spacer can be hydrophobic, hydrophilic, short or long, rigid or flexible (62). The most widely investigated GS are the quaternary ammonium *m-s-m* type in which *m* represents the number of carbon atoms in the alky tail groups and *s* is the number of carbon atoms in a polymethylene spacer. There are numerous other examples of GS including anionic, cationic, zwitterionic, and non-ionic, with a wide variation in the type of head group, the length and composition of the spacer group, and the length of the alkyl tail groups (62). As the structure of GS is flexible, it is easy to choose two identical or different amphiphilic molecules and link them with a desired spacer group.

Since gemini surfactants have specific self-assembly abilities, they have much more important characteristics than conventional monomeric surfactants. Some distinctive features of gemini surfactants are: considerably low cmc values compared to monomeric surfactant, high surface activity, low Kraft temperature, ability to form a wide range of aggregate structures, and better wetting ability (50).
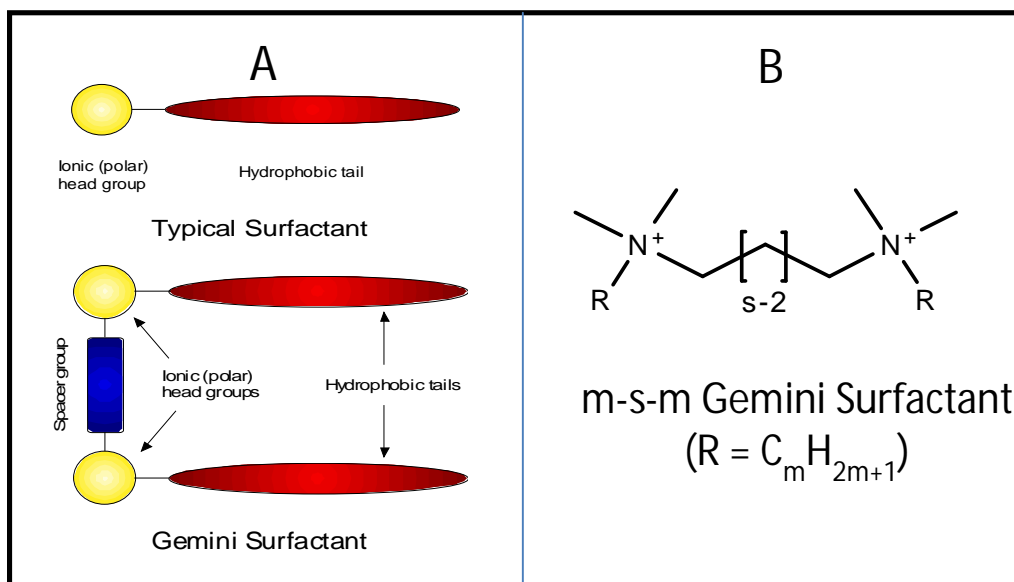
Figure 1.4.1:Gemini surfactant structure. A) Structural similarity and contrast between typical surfactant monomer and Gemini surfactant monomer. B) General structure of m-s-m Gemini surfactant. Adapted from (63).

1.4.1 Gemini surfactant structure and aggregation properties

Changes in gemini surfactant structure can affect their behaviour in solution and interactions with polymers and biomacromolecules. For instance, the addition of hydrophilic groups in the spacer increases the hydrophilicity of the molecules, or gemini surfactants can become more water soluble if their alkyl chain carbon number decreases (62).

As Aβ is a peptide containing various amino acids, its structure can be affected by gemini surfactants. Diversity in the gemini surfactants' structure is helpful in determining the nature of interactions between gemini surfactants' different parts and Aβ. If it is observed that the hydrophobic part of gemini surfactant is more important in interaction with Aβ than the spacer

17

group, the attempts will be focused on the alkyl tail group and its hydrophobic properties in interaction with Aβ. Thus, variation in gemini surfactant structure can be helpful in leading researchers to the optimum structures in interaction with Aβ and preventing Aβ aggregate formation.

1.4.1.1 Effect of the spacer

The aggregation properties of gemini surfactant are affected by inter-molecular and intra-molecular interaction of gemini surfactant molecules as well as their interaction with solvents. As it was mentioned in the previous section, gemini surfactant has a spacer which plays a critical role in gemini surfactant's characteristics. The spacer can be used to control the hydrophobic interactions. The spacer group can also be effective in manipulating the electrostatic repulsion between gemini surfactant's charged head groups (50). The nature of the spacer does not have a significant impact on the cmc of gemini surfactant. Hence, based on the expected physical or biological properties, the spacer can be changed without a substantial change in the cmc of gemini surfactant (64).

1.4.1.2 Effect of the alkyl tail group

The intra and inter molecular hydrophobic interactions between alkyl chains of gemini surfactants play an important role in gemini surfactant's characteristic (50). The length of the tail group affects cmc (Figure 1.4.1.2.1). There is a linear correlation between the number of carbon in the alkyl chain (up to m=16) and ln(cmc) for m-2-m, m-3-m, m-5-m, m-6-m. Linear correlation between alkyl tail carbon number and ln(cmc)can be observed in m-4-m up to m=18.

It was also observed that for m-6-m (m=7,8,9,10,11,12,16) the enthalpy of micellization for even numbered alkyl chain have different exothermic and endothermic values whereas for odd numbered alkyl chain the enthalpy of micellization values are all endothermic. The difference in the enthalpies arises from the various conformations of gemini surfactant molecules with even and odd alkyl chains (65).
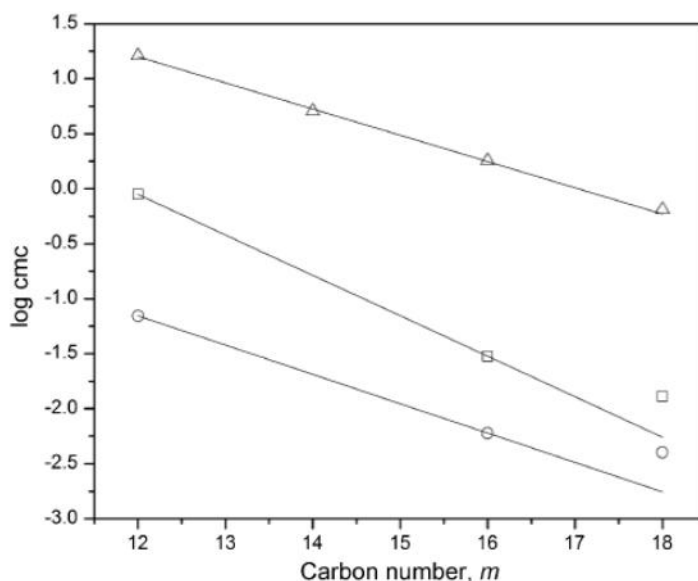
Figure 1.4.1.2.1.Variation of the logarithm cmc as a function of alkyl tail length for the gemini surfactants: m-3-m (□); phy-3-m (○); m-6-6 (△). Adapted from (66).

1.4.2 Gemini surfactant interaction with biomacromolecules

As mentioned earlier, gemini surfactants' specific properties make them a target for biological and biomedical applications. In biology, the safety of compounds has a critical importance. The lower cmc of gemini surfactants compared to conventional ones permit usage in lower quantities than conventional surfactants. Thus, the amount of surfactant used in biological

research is low enough to meet the safety issues (50). The complexity of gemini surfactant interaction with biomacromolecules are more than gemini surfactant/polymer system. The reason is related to the different possible interactions between gemini surfactant and biomacromolecues (electrostatic, hydrophobic and hydrophilic interaction, hydrogen bonding). The interaction between gemini surfactant and biomacromolecules may cause change in aggregation properties, morphology and structure of biomacromolecules. The bioactivity of biomacromolecules can be affected by the gemini surfactant as well. Therefore, better understanding of gemini surfactant-biomacromolecule interaction can be helpful in optimizing the surfactant-biomacromolecule systems (50).

Among the biomacromolecules, DNA is of interest for the purpose of gene therapy. Different studies have been done to evaluate the effect of the different gemini surfactants in compacting DNA and non-viral delivery systems (67-69). Another important macromolecule is Aβ. Different research focused on the effect of surfactants on disaggregation of Aβ aggregates (70-72).

1.4.3 Aß and surfactant interaction

Surfactants are the effective reagents that can be used in disaggregation of Aβ aggregates and in preventing Aβ fibrillogenesis. It has been observed that sodium dodecyl sulfate (SDS) micelles prevent Aβ(1-40) monomers aggregation and thus amyloid fibril formation stopped (73,74). Hexadecyl-N-methylpiperidinium (HMP) bromide is the other surfactant that has inhibitory effect on Aβ peptide aggregation (75). The inhibitory effect of surfactants depends on their concentration. Sabaté et al. compared the effect of alkyl bromides in different

20

concentrations. They observed that in concentrations lower than alkyl bromides cmc, the Aß fibril formation was promoted whereas in concentration above cmc, the micelles form and cause prevention of Aß aggregate formation (36).

1.4.4 Aß and gemini surfactant interaction

Gemini surfactants can affect Aβ aggregation because of their specific structure. The effect of gemini surfactants on Aβ aggregation was studied by Wang et al. (2006). They used gemini surfactant 12-6-12 and compared its effect with DTAB (dodecyl trimethyl ammonium bromide). According to their research, both 12-6-12 and DTAB caused rapid aggregation of Aβ at first. Then the surfactant's head groups repulsive force causes Aβ fibril disruption. 12-6-12 has stronger effect on AB dissociation in lower concentration than DTAB (76). In a solution containing Aβ aggregates, addition of gemini surfactant results in attachment of these molecules to Aβ aggregates. In this stage dehydration of Aβ aggregates occurs that leads to the formation of condensed Aβ aggregates. The Aβ molecule has slightly negative charge in pH=7.4 because of having Asp, Glu in its side chain. Electrostatic interactions and neutralization occur between the cationic gemini surfactant and the negatively charged Aβ aggregates. All these circumstances lead to the formation of more condensed Aβ aggregates. With the addition of more surfactant, Aβ dehydration takes place, which leads to Aβ condensation. This dehydration occurs due to neutralization of Aβ aggregates by cationic surfactant molecules, which results in displacement of water molecules (that were previously shielding the repulsive force between same-charged chemical groups in Aβ). In fact, the surfactant molecules on the Aβ aggregates affect the intra-peptide interactions between Aβ aggregates. The hydrophobic alkyl tail of the surfactant can

interact with the hydrophobic portion of Aβ amino acids. These hydrophobic interactions also contribute to the formation of surfactant-Aβ aggregates. The formation of gemini surfactant-Aβ aggregates is faster and stronger than conventional surfactant-Aβ aggregates since gemini surfactants have two charged head groups and two hydrophobic tail groups, which are important in interaction with Aβ aggregates (76). After reaching this point, the addition of more surfactant molecules causes an increase in the positive charge on Aβ aggregates. Then the repulsive force between the surfactant's head groups increases and the Aβ aggregates are disrupted (76). After Aβ aggregate dissociation, the Aβ and gemini surfactants reassemble to make spherical mixed micelles (Figure 1.4.4.1).
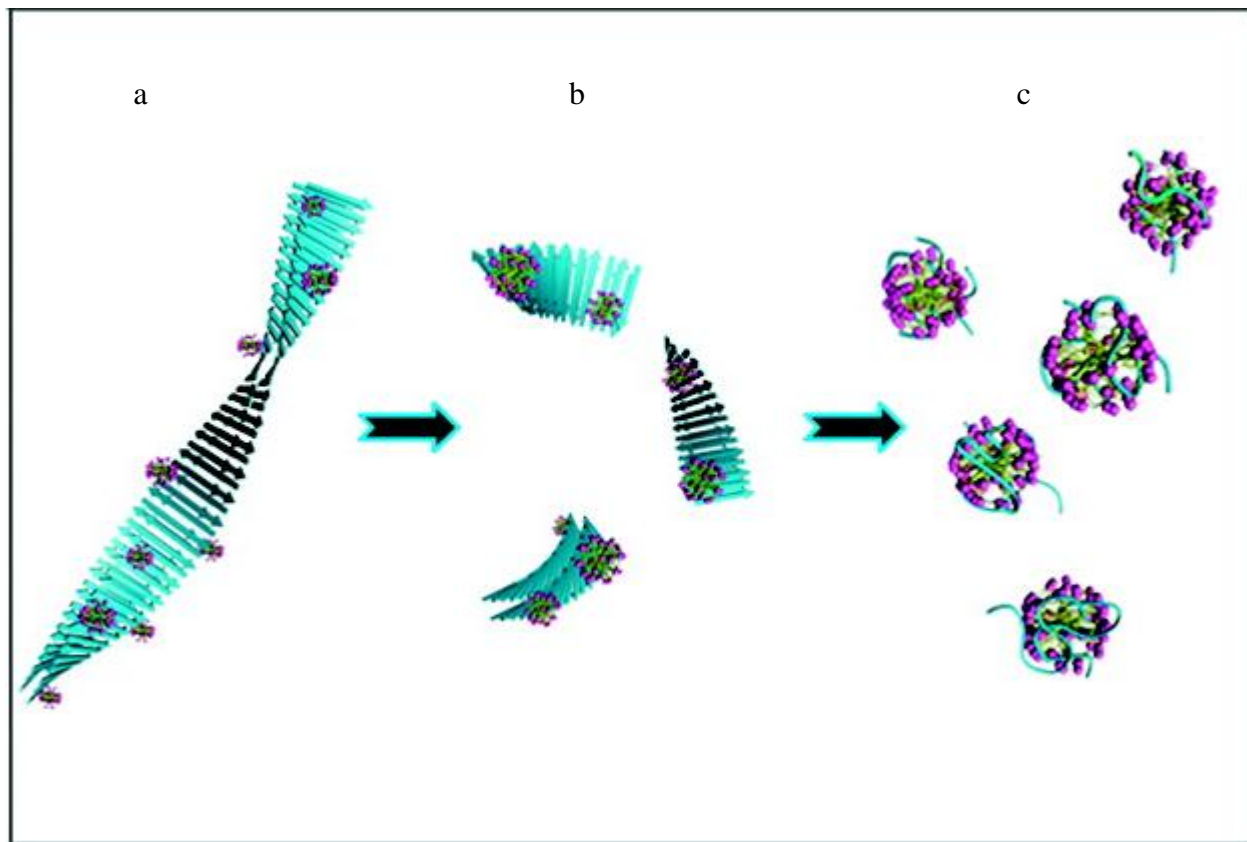
Figure 1.4.4. 1: Mechanism of the 12-6-12 micelles disassembling the Aβ(1−40) fibril. (a) Binding of the C12C6C12Br2 micelles onto the fibril surface. (b) Breaking down of a long fibril into short pieces. (c) Complete disassembly of fibrils and the formation of mixed aggregates (72).

1.5 Objectives of the proposal research

Hypothesis statement: *the spacer structure of a gemini surfactant, including it's hydrophilicity, will increase the disruption of amyloid ß peptide aggregates.*

Short term objective:

1-To evaluate the cmc and cac of the gemini surfactant with Aß peptide using the surface tensiometry technique.

2-To determine the possible interactions of gemini surfactants with different spacer groups with amyloid ß aggregates, by using isothermal titration calorimetry.

3- To use dynamic light scattering to evaluate the change in particle size of Aß in different surfactant concentrations.

Significance of the work: Gemini surfactants may be useful as drug delivery systems for the delivery of drug's in Alzheimer's disease. My work also suggests that gemini surfactants may disaggregate Aß peptide clusters and may directly help in the treatment of Alzheimer's disease.

Chapter 2: Experimental procedures

2.1 Materials

The Gemini surfactant that has been previously examined with respect to Aß aggregation is the 12-6-12 surfactant (72, 76, 77). There are various GS that can be used to determine their effect on Aβ aggregation. We expanded this work using our library of GS previously synthesized (78-81) to determine structure-activity relationship(s) for Aß fibril disintegration. GS that were used: 12-2-12 (82), 12-3-12, 12-4-12, 12-7-12 (82), (12-5N-12, 12-8N-12,)(83), (12-4(OH)-12, 12-4(OH)$_2$-12)(81),12- EO- 12,12-EO$_2$-12, 12-EO$_3$-12(80) (Figure 2.1.1). All GS solutions were prepared in Milli-Q ultrapure water and then filtered through 0.22 μm filters.

Amyloid beta peptide (1-42) was obtained from rPeptide (Bogart,Georgia, USA). The peptide purity was > 97%. Preparation of Aβ (1-42) is by addition of hexafluoroisopropanal (HFIP) to the Aß(1-42) stock, then the solution of Aß and HFIP was aliquoted into microcentrifuge tubes. Then the microcentrifuge tubes containing HFIP and Aß were left in room temperature until HFIP evaporated completely. After that, the tubes containing peptide were stored at -20℃. Thirty minutes before each experiment, fresh milli Q water was added to the centrifuge tubes to make Aβ (1μg/ml) solution. Milli-Q water obtained for this study was from Millipore synergy purification system.
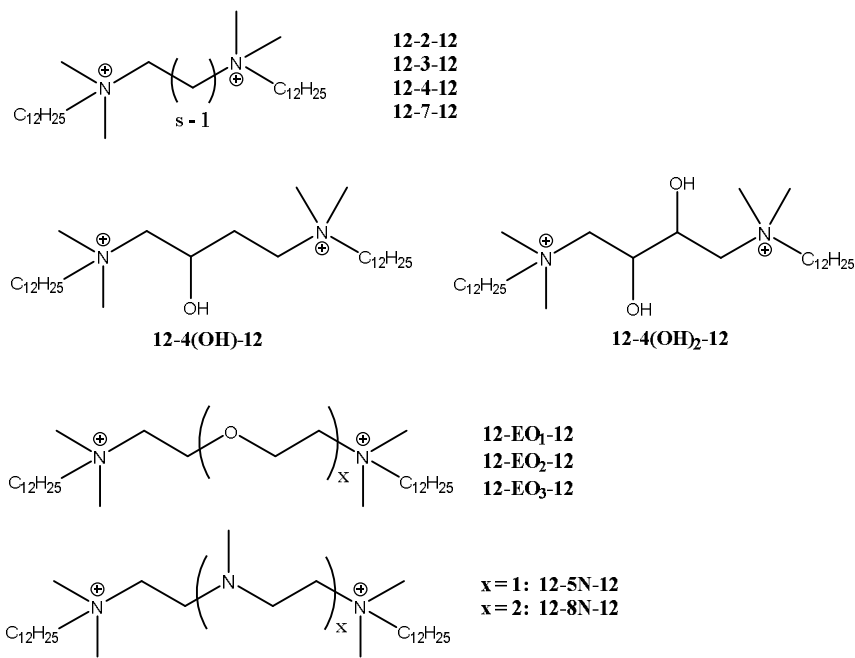
Figure 2.1.1: Structure of the amine-substituted Gemini Surfactants. Adapted from (81)**.**

2.2 Method

2.2.1 Surface tension measurements:

For determining cac and cmc of surfactant-Aβ solutions, surface tension was measured using a Lauda model TE3 automated tensiometer (Lauda, Germany) by the due Nouy ring method. The surface tension was measured after each titration of gemini surfactant 10 mM and 1 mM solutions in Aβ (1μg/ml) solution at 25.0°C.

2.2.2 Isothermal titration calorimetry

Isothermal titration calorimetry (ITC) is a useful technique for evaluating the binding energetic of biological processes such as protein-protein binding, protein-carbohydrate binding, protein-lipid binding, antigen-antibody binding, DNA-protein binding and Aβ-surfactant binding.

ITC method can be used to determine the stability constants, stoichiometry, interaction enthalpies, entropies, Gibbs free energies and heat capacity changes. Therefore, it can be a method of choice in different areas of study such as biological and bio-molecular interactions, ligand binding, enzyme activity, biotechnology, drug discovery, protein-protein interaction, etc (84).

The advantage of titration calorimetry is that binding isotherms determine the heats of reaction that can estimate the enthalpy changes and heat association constant. As such, using calorimetric titration defines the characterization of the energetic of binding. In an ITC experiment the titrant is added to a sample solution at a constant temperature. The heat released or absorbed in each addition can be provided by ITC (84).

In polymer surfactant interaction, ITC is one of the most sensitive methods that can measure thermodynamic changes. In charged polymers and charged surfactants category, the electrostatic forces play a critical role. When polymer and surfactant molecules in opposite charges are neutralized, the excess surfactant can re-solubilize the precipitated polymer-surfactant aggregates. Calorimetry can be used to measure the heat of interaction (or molar enthalpy ΔH) directly. When two molecules bind, heat can be released or absorbed. Isothermal

27

microcalorimetry is a technique that can be used for measurement of heat released or absorbed in biomolecular interactions.

An ITC instrument consists of two cells (sample cell and reference cell) that are made from highly efficient thermal conducting material (Figure 2.2.2.1). The cells are surrounded by an adiabatic jacket. A circulating water bath can be used to cool down the jacket.

The molecular interaction between two molecules is defined by the following equation:

$$\Delta G = -RT \ln K_A = \Delta H - T\Delta S \qquad (2.1)$$
$$ a b$$

In part a, Gibbs free energy (ΔG) correlates with association constant K_A, since R (gas constant), and T (absolute temperature), are constant. Part b in equation 2.1 shows the sum of enthalpy (ΔH) and entropy (ΔS) changes that explain the free energy (ΔG) and tendency of molecules for interaction. In ITC experiment, both K_A and ΔH can be measured. Therefore, the other parts (ΔG and ΔS) of equation 2.1 can be derived from K_A and ΔH (85).
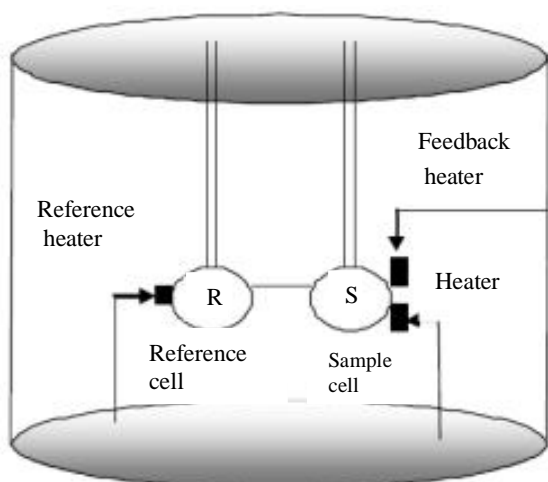
Figure 2.2.2.1: Schematic diagram of an ITC instrument

ITC is sensitive to thermodynamic change in polymer- surfactant interaction. The non covalent force between the surfactant and polymer helps us to understand the interaction mechanism between polymer and surfactant molecules (61).

ITC measurements were carried out using a MicroCal VP-ITC calorimeter. Aliquots of gemini surfactant (10mM) were injected from a Hamilton syringe into the sample cell containing Aβ(1μg/ml). For each gemini surfactant two experiments were performed, the same procedure was performed with water in the sample cell as a reference. For each ITC experiment the injection parameters were as follows: initial delay 60 sec, duration of each injection 4 sec, interval between two injections 240 sec, filter period 2 sec. A combination of 5 µL, at low surfactant concentrations, and 10 µL, at higher concentrations, were used for the titration of concentrated surfactant solution into the titration cell. The experimental temperature was at 25°C± 0.05°C. The results of ITC experiments were analyzed using Origin® scientific plotting software, version 7.0, and excel Microsoft, version 2007 software.

2.2.3. Particle size measurement

Particle size measurements were performed on a Malvern Zetasizer Nano ZS instrument (Malvern Instruments, Worcestershire, UK) in a cell connected to a titration module. In forward titrations, 10 mM gemini surfactant was titrated into Aβ (1μg/ml) solution. Individual particle size measurements were performed using quartz cells. To determine the size distribution non-negative least squares (NNLS) analysis method was used (scattering was determined at θ = 173°). The intensity and volume of particles were reported. For each data, particle size measurement was repeated five times and the average is reported.

Chapter 3: Results and Discussion

3.1 Surface tension studies of the gemini surfactants / Aβ systems.

Surface tensiometry is a powerful tool for the study of the aggregation behavior of surfactants in the presence of additives, particularly additives such as polymers or peptides. As introduced in Section 1.3.2, the addition of a polymer to a surfactant solution is expected to result in aggregation of the surfactant at a critical aggregation concentration (cac; equivalent to T_1 in Figure 1.3.2.1). The aggregation of surfactant and Aß is due to the favorable interactions between the polymer and surfactant. The cac is typically at some concentration lower than the cmc for the surfactant in water alone. This is followed by saturation of the polymer with surfactant and eventually any added surfactant will form regular surfactant micelles (T_2 and T_3 in Figure 1.3.2.1, respectively).
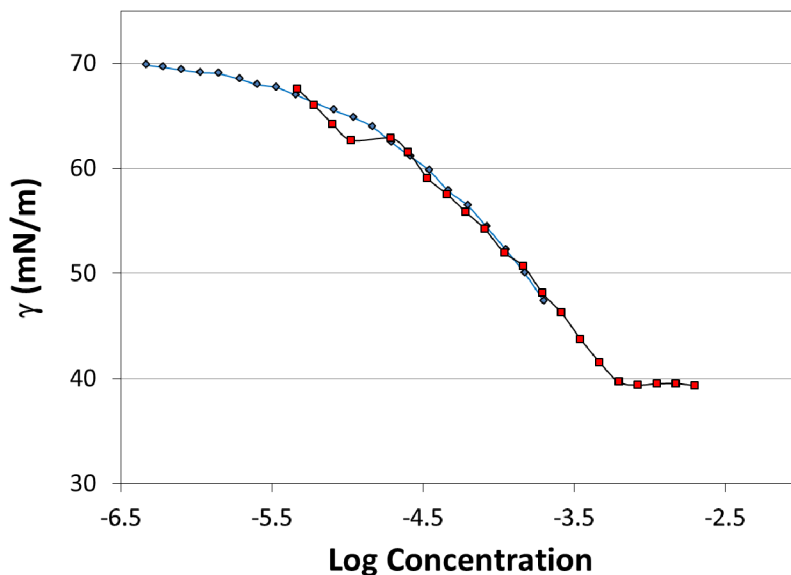
Figure 3.1. 1. Surface tension plot for the titration of the 12-8N-12 gemini surfactant (◆ = 1 mM stock solution; ■ = 10 mM stock solution) into a 1μg/mL solution of Aβ in water.

A representative example of the surface tension behavior for the gemini surfactants in the presence of Aβ, is presented in Figure 3.1.1. Plots of the surface tension for the remaining surfactants with Aβ are provided in Appendix 1. In Figure 3.1.1, it is observed that at low surfactant concentrations, the surface tension is approximately equal to 70 mN/m, equivalent to that of pure water at $25.0\ ^{\circ}\mathrm{C}$. As the concentration of surfactant is increased, we see no evidence of the expected cac, T_2 or T_3 critical concentrations. Instead, a reduction in the critical micelle concentration from 1.10 mM in water to 0.62 mM in the presence of Aβ is observed (see Table 3.1.1). This suggests that Aβ is not behaving as a neutral polymer as expected, but rather as a hydrophobic solute that induces micelle formation at a substantially lower concentration as a

31

means of removing itself from unfavorable contacts with water, and forms mixed micelles with the gemini surfactants.

The above results are consistent with the observations of Li et al. (76) who observed the formation of small, globular aggregates of approximately 10 – 15 nm in size for the 12-6-12/ Aβ system using AFM. It is worth mentioning that the concentrations of Aβ used in their study were significantly higher than those used in this work. Nevertheless, our interpretation of the formation of mixed micelles of gemini surfactant and Aβ is consistent with their results.

Table 3.1.1: Critical micelle concentrations (cmc) and head group areas (a_0) obtained from surface tension measurements for the gemini surfactants in water and in 1 μg/mL Aβ in water solutions. Values in water are from literature sources.

Surfactant	cmc_{water} (mM)	$cmc_{A\beta}$ (mM)	$a_{0,water}$ (nm^2)	$a_{0,A\beta}$ (nm^2)
12-2-12	0.86 ± 0.08[a]	0.66 ± 0.06	0.86 ± 0.05 [a]	0.97 ± 0.02
12-3-12	0.89 ± 0.13 [a]	0.86 ± 0.13	1.11 ± 0.04 [a]	1.06 ± 0.11
12-4-12	1.1 ± 0.1 [a]	1.08 ± 0.04	1.15 ± 0.09 [a]	1.36 ± 0.03
12-7-12	0.85 ± 0.07 [b]	0.70 ± 0.07	1.24 ± 0.06[b]	1.85 ± 0.08
12-4(OH)-12	0.85 ± 0.18[c]	0.83 ± 0.04	1.19 ± 0.08[c]	1.22 ± 0.02
12-4(OH)$_2$-12	0.75 ± 0.15[c]	0.41 ± 0.04	1.15 ± 0.04[c]	0.99 ± 0.05
12-EO$_1$-12	0.84 ± 0.04[d]	0.75 ± 0.14	1.12 ± 0.03 [d]	0.73 ± 0.08
12-EO$_2$-12	0.86 ± 0.04 [d]	0.74 ± 0.14	1.33 ± 0.08 [d]	2.02 ± 0.07
12-EO$_3$-12	1.10 ± 0.05 [d]	0.75 ± 0.19	1.75 ± 0.09 [d]	2.39 ± 0.08
12-5N-12	1.14 ± 0.04[e]	0.68 ± 0.10	1.30 ± 0.03 [e]	1.01 ± 0.02
12-8N-12	1.10 ± 0.10 [e]	0.62 ± 0.03	1.95 ± 0.13 [e]	1.74 ± 0.04

[a] From reference (82)
[b] From reference (86)
[c] From reference (81)
[d] From reference (80)
[e] From reference (83)

The head group areas (a_0), (Table 3.1.1) for the gemini surfactants were calculated according to Equation 3.1:

$$a_0 = (N_A \Gamma)^{-1} \quad 3.1$$

where Γ is the Gibbs surface excess concentration for the surfactant at the air water interface, which is calculated from the slope of the surface tension curve ($\delta\gamma/\delta\log C$), just prior to the cmc, according to Equation 3.2:

$$\Gamma = -\frac{1}{2.303nRT}\left(\frac{d\gamma}{d\log C}\right)_T \quad 3.2$$

where R and T have their usual meaning, and n is a constant accounting for the dissociation of ionic surfactants; for the gemini surfactants n = 3 (81). Comparing a_0 for the 12-s-12 surfactants in the presence of Aβ to those obtained in water we see a decrease in a_0 of some of the GS in the presence of Aβ. This likely results from a relaxation of the electrostatic repulsion between adjacent surfactant molecules as a result of the incorporation of Aβ chains. It may also be the case that the amino acid residues within the Aβ peptide chains partially neutralize the charge on the gemini surfactant molecules themselves, through electrostatic interactions with the surfactant head groups, further relaxing electrostatic repulsion. No clear pattern is observed for the substituted gemini surfactants, regardless of the nature of the substituent group. However, the addition of substituent groups within the spacer of the gemini surfactants affects their ability to interact with Aβ, which means that the head group structure is important in surfactant/Aβ interaction. It is worthy to note that some of the GS showed an increase in the a_0 in the presence of Aß which might be due to other interactions rather than the electrostatic interaction. To obtain

a better understanding of how surfactant structure impacts these interactions we undertook a titration calorimetry and dynamic light scattering study, described in Section 3.2 below.

3.2 Gemini surfactant-Aß interaction: ITC and particle size measurement

The interaction between the gemini surfactants and Aβ has been examined in more details using ITC and particle size measurements. For better understanding of the results obtained, and the importance of changes within the molecular structure of the surfactants, the type of interactions that may occur between the surfactant and the Aβ peptides should be considered. The possible interactions that can occur include:

1. Hydrophobic interactions between peptide and surfactant molecules

2. Hydrophobic interactions between surfactant molecules

3. Hydrophobic interactions between peptide molecules

4. Electrostatic interactions between peptide and surfactant molecules (may be attractive OR repulsive)

5. Electrostatic interactions between surfactant molecules (Repulsive)

6. Electrostatic interactions between peptide molecules (may be attractive or repulsive depending upon pH, amino acid sequence, etc.) (87).

In this work, we decided to focus on variations in the structure of the head group of the surfactant, the rationale for which was the idea that electrostatic interactions between the surfactant head group and the amino acids in the Aβ peptide are potentially more important in the interaction as compared to hydrophobic interactions (76,81). Nevertheless, the observed

differences in binding, described below, will involve changes in electrostatic interactions, weaker interactions arising from hydrogen bonding, and changes in the hydrophobic nature of the spacer group of the GS. As such, with the help of particle size data also presented below, we will interpret the binding observed in our calorimetric studies on the basis of the above contributions to the complete binding interaction.

The enthalpograms for the titration of each gemini surfactant into water, and into a 1µg/ml solution of Aß are shown in Figures 3.2.1 to 3.2.4. From these figures, it is apparent that marked differences occur for some of the surfactants, suggesting stronger interactions with Aß, depending upon head group structure. As observed in Section 3.1 in our surface tension
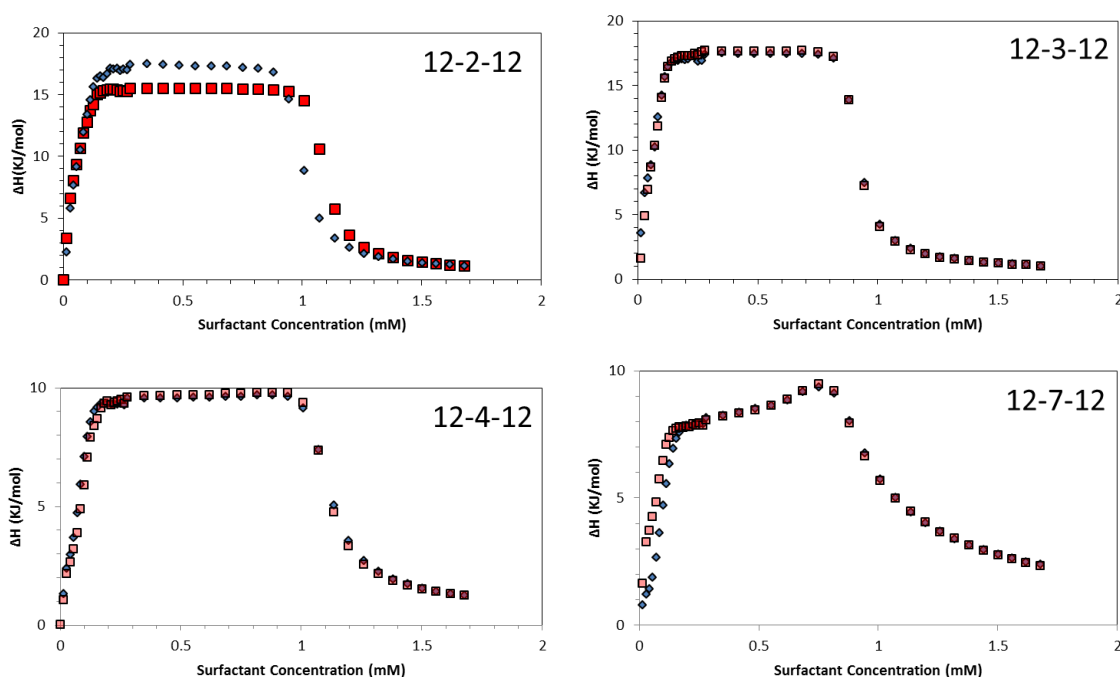
Figure 3.2.1: Observed enthalpies for the addition of un-substituted gemini surfactants in water(◆), and in Aß (1µg/ml) solution(■).

35
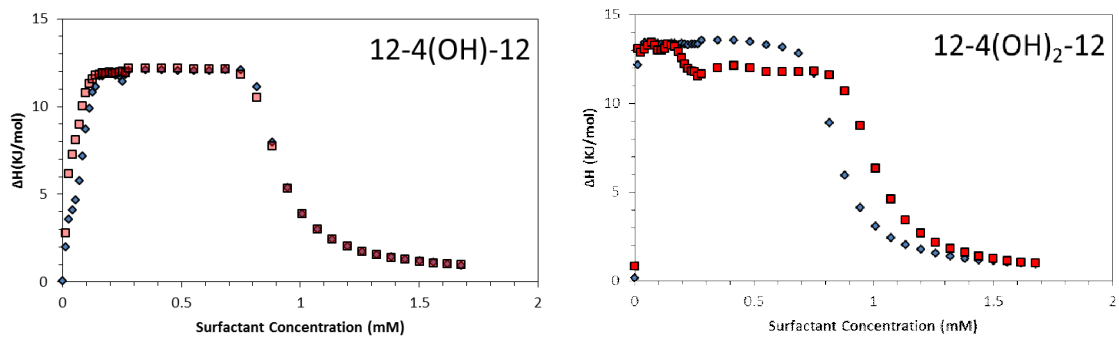
Figure 3.2.2: Observed enthalpies for the addition of hydroxyl-substituted gemini surfactants in water(◆), and in Aß (1μg/ml) solution(■).
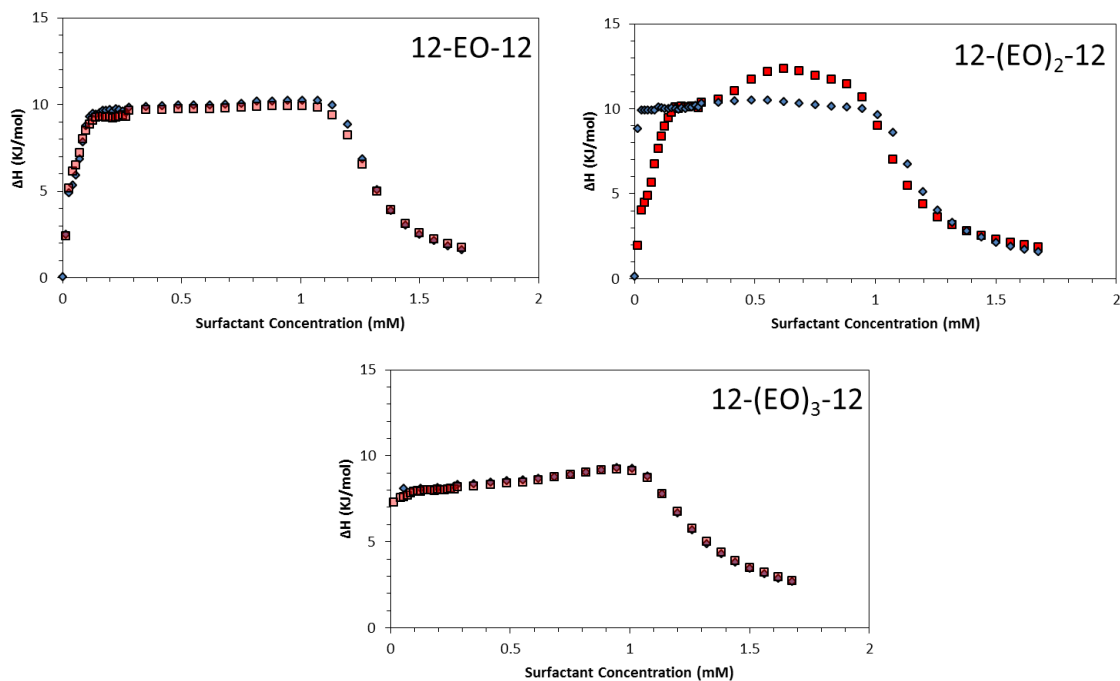
Figure 3.2.3: Observed enthalpies for the addition of ethoxyl-substituted gemini surfactants in water(◆), and in Aß (1μg/ml) solution(■).
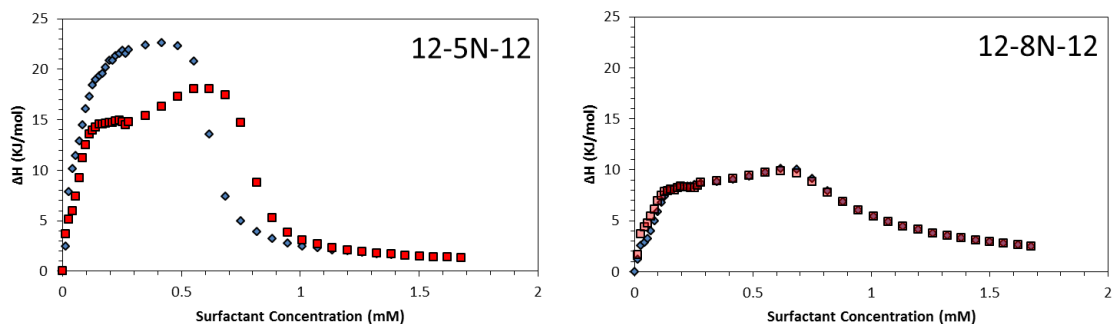
Figure 3.2.4: Observed enthalpies for the addition of amine-substituted gemini surfactants in water(◆), and in Aß (1μg/ml) solution(■).

measurements, little difference is observed in the enthalpograms, generally, when Aß is added to the system. Then enthalpograms look very similar to those obtained for the titration of each surfactant into water alone, and the data supports the interpretation that Aß is behaving as a hydrophobic solute and the interaction of the surfactant is one of mixed-micelle formation, rather than a "typical" surfactant polymer/peptide interaction (as such interactions were introduced in Chapter 1). CMC values and enthalpies of micellization (ΔH_{mic}) have been determined for each surfactant for the titration into water (CMC_{aq}, $\Delta H_{mic, aq}$) and into Aß solution ($CMC_{Aß}$, $\Delta H_{mic, Aß}$) and are listed in Table 3.2.1.

Table 3.2.1: Critical micelle concentrations (CMC) and enthalpies of micellization (ΔH_{mic}) obtained from ITC measurements for the gemini surfactants in water and in 1 μg/mL Aβ in water. Values in parentheses are literature values.

Surfactant	CMC_{aq} (mM)	$CMC_{Aß}$ (mM)	$\Delta H_{mic, aq}$ (kJ mol^{-1})	$\Delta H_{mic, Aß}$ (kJ mol^{-1})
12-2-12	1.09	1.18	-15.5 (-22[a])	-14.1
12-3-12	1.03	1.03	-16.0	-16.1
12-4-12	1.23	1.21	-8.3 (-9.3 [a])	-8.5
12-7-12	1.12	1.04	-6.9	-7.0
12-4(OH)-12	1.02	1.03	-11.0 (-12.1[b])	-10.8
12-4(OH)$_2$-12	0.98	1.14	-11.8 (-11.5[b])	-10.5
12-EO$_1$-12	1.38	1.39	-8.4 (-13.3[c])	-7.9
12-EO$_2$-12	1.26	1.18	-8.3 (-9.9[c])	-9.5
12-EO$_3$-12	1.34	1.34	-6.4 (-9.2[c])	-6.4
12-5N-12	0.73	0.92	-20.9 (-11.9[c])	-16.7
12-8N-12	1.09	1.18	-15.5 (-3.0)	-14.1

[a] From reference (88)
[b] From reference (81)
[c] From reference (80)
[d] From reference (83)

Very good agreement is seen between $\Delta H_{mic, aq}$ obtained in this work, and those reported in the literature, as well as between aqueous CMC values obtained from ITC and surface tension measurements; observed differences are typical of those seen for measurements made using different instruments (ITC values) or different methods (i.e., surface tension vs ITC). The differences observed for the titration of surfactant into water as compared to Aß solution are small, and the interpretation is not as clear as for the surface tension study. Nevertheless, the magnitudes of the CMCs and enthalpies of micellization are very similar, and support a solubilization process as compared to a binding interaction for the mixed surfactant/Aß system.

That said, any differences in the enthalpograms are difficult to interpret as presented in Figures 3.2.1 to 3.2.4. In order to provide a better discussion, the differences in observed enthalpy (ΔH) were determined, and these results are described in further detail in the following sections.

3.2.1 Interactions between the un-substituted (12-s-12) gemini surfactants and Aβ

Figures 3.2.1.1 shows subtracted enthalpies (ΔH) and the particle sizes (diameter) as a function of surfactant concentration for the 12-s-12 / Aβ systems. The subtracted enthalpy profiles are obtained by subtracting the observed enthalpies for the titration of the surfactant into water ($\Delta H_{obs, water}$) from the observed enthalpies for the titration of the surfactant into Aβ solution ($\Delta H_{obs, A\beta}$), i.e.:

$$\Delta H = \Delta H_{obs,A\beta} - \Delta H_{obs,water} \qquad \text{Eqn. 3.1}$$

where ΔH_{obs} is the sum of the enthalpy of dilution of gemini surfactant solution in Aß solution, dilution of gemini surfactant micellar solution, dehydration of Aß peptide aggregates, reformation of Aß aggregates and Aß/gemini surfactant interaction; i.e.,

$$\Delta H_{obs} = \Delta H_{demicellization} + \Delta H_{dilution} + \Delta H_{dehydrationA\beta} + \Delta H_{A\beta \text{ aggregate reformation}} + \Delta H_{surfactant-A\beta}. \quad \text{(Eqn. 3.2)}$$

Subtracted enthalpies are useful to observe the small differences between the enthalpies and provide better details to discuss about the possible interaction between gemini surfactants and Aß. Different behavior is observed for these surfactants, depending upon the length of the spacer group, s = 2, 3, 4, or 7. These 4 surfactants were chosen because of their relation to the various substituted surfactants: 12-2-12 corresponds to 12-EO$_0$-12 and the parent surfactant for the 12-5N-12 and 12-8N-12 surfactants; 12-4-12 is the parent surfactant for the 12-4(OH)$_X$-12, and 12-
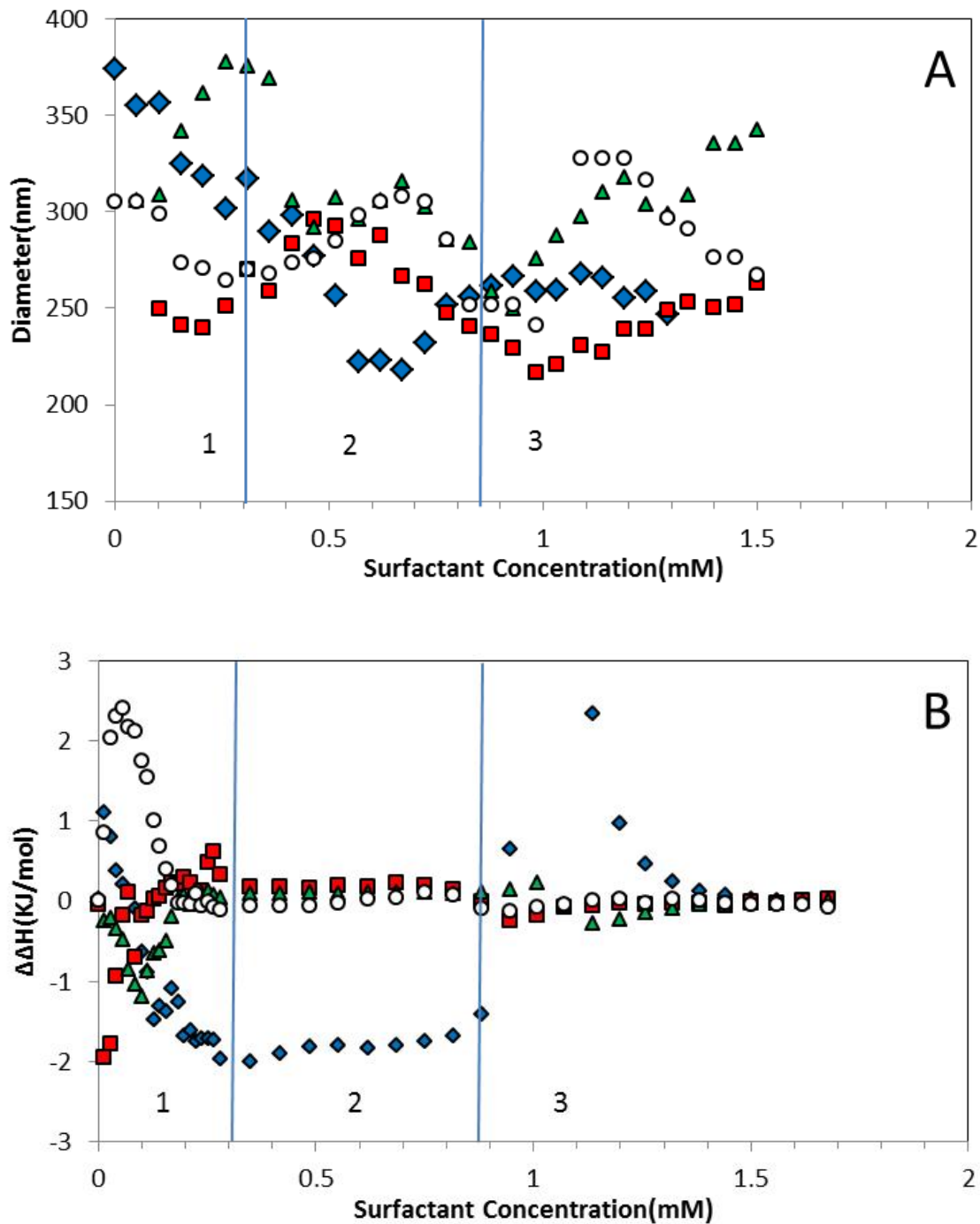
Figure 3.2.1.1. A) Dynamic light scattering and B) Observed enthalpies for the addition of 12-2-12 (◆), 12-3-12(■), 12-4-12 (▲) and 12-7-12 (O) into Aß (1µg/ml) solution.

3-12 and 12-7-12 provide a more complete series of the 12-s-12 surfactants.

Examining the particle size and enthalpy data, we can define 3 distinct regions to the interaction(s), as a function of surfactant concentration. In the absence of added surfactant, the Aβ peptide has an average particle size of ~300 nm, with a large degree of variability (see the 0 added surfactant data points in Figures 3.2.1.1 A). Upon addition of surfactant the average particle sizes are, generally, observed to decrease with the exception of 12-4-12 surfactant, which is observed to increase in particle size, initially. At the same time the enthalpies are observed to generally decrease (i.e. an exothermic transition), this time with the exception of the 12-3-12 surfactant (initial endothermic increase in enthalpy is observed for 12-3-12). The addition of the gemini surfactants to water initially results in a demicellization of the concentrated surfactant, which causes an increase in enthalpy that is, for 12-s-12 surfactant series, observed to be strongly endothermic in nature. This is in agreement with the observations made by Li et al (76) for the 12-6-12 surfactant, although it should be noted that their study was carried out at a significantly larger Aβ concentration (0.116 mM) which may account for the much larger changes observed in their study.

The addition of the gemini surfactant to Aβ results in a neutralization of the overall negative charge carried by Aβ at neutral pH (approximately 6 at neutral pH (76). This results in a relaxation of the peptide, promoting further association of the surfactant with Aβ and reducing unfavorable interactions with water and the neutralized, hydrophobic, Aβ. This results in a dehydration of both Aβ and the gemini surfactant, and a substantial exothermic contribution to the enthalpy, as observed in Figure 3.2.1.1 B.

41

It is interesting to note, that very different behavior can be observed in both the particle size and enthalpy profiles (Figures 3.2.1.1 A and B, respectively) depending upon the length of the polymethylene spacer, i.e., s = 2, 3, 4, or 7. If we expand Region 1 in Figure 3.2.1.1 B (see now Figure 3.2.1.2) we can observe that for both the 12-3-12 and 12-7-12 surfactants, the first additions of surfactant result in an **increase** in enthalpy (endothermic), and then decrease in enthalpy back to approximately zero. This is in contrast with the 12-2-12 and 12-4-12 surfactants for which the enthalpy decreases immediately upon addition of surfactant (i.e. exothermic). This difference is attributable to the differences in the ability of the hydrophobic tails to rotate around the spacer group, specifically for short spacer groups, as a result of steric hindrance (88).

The particle size data generally supports the above interpretation, as Aβ is dehydrated, it can be compacted by the added surfactant, resulting in an overall decrease in particle size, as seen in Figure 3.2.1.1 A. Unfortunately, because of a great fluctuation in size data (resulting from the large heterogeneity observed in measured particle sizes) making any additional conclusions about binding between the 12-2-12/Aß, 12-3-12/Aß, 12-4-12/Aß, and 12-7-12/Aß surfactants systems are difficult. AFM and EM are useful techniques to assess the size and shape of the surfactant/Aß particles to confirm our interpretation.
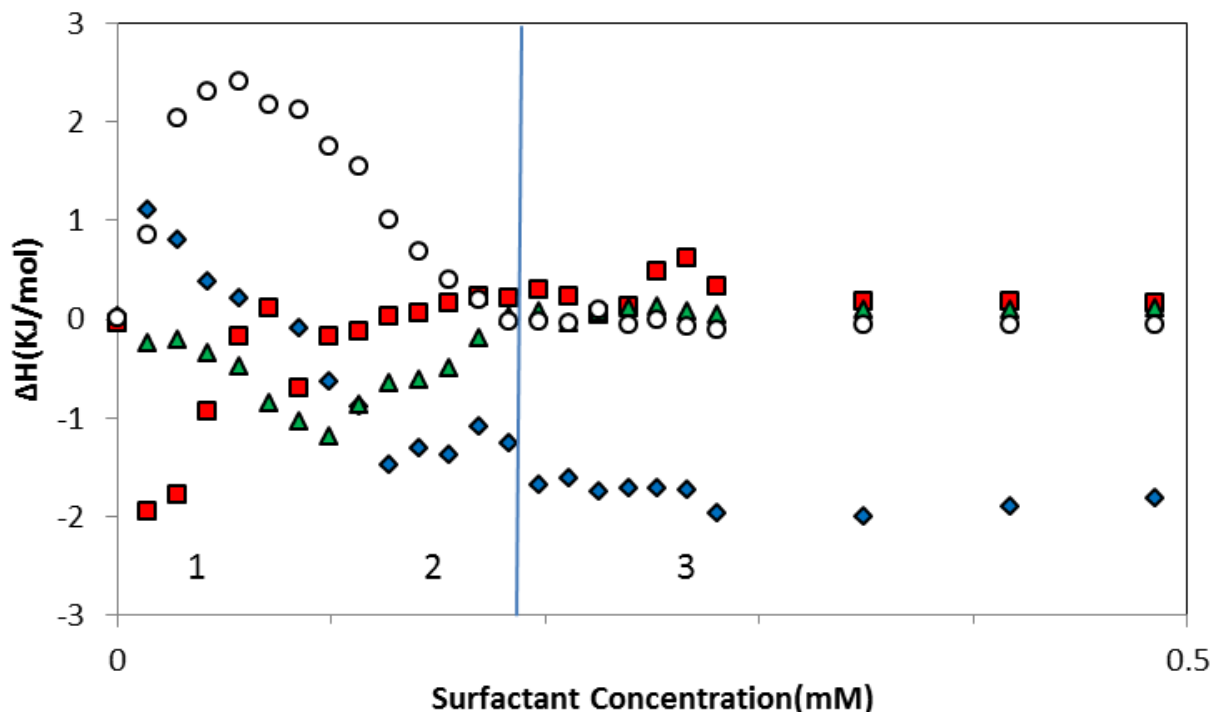
Figure 3.2.1.2.Expanded enthalpy profile for the the addition of 12-2-12 (◆), 12-3-12(■), 12-4-12 (▲) and 12-7-12 (O) into Aß (1µg/ml) solution.

Looking now at region 2, for all 3 surfactants there is a flattening of the enthalpy profile (Figure 3.2.1.1 B), with the observed enthalpy being approximately zero for the 12-3-12, 12-4-12, and 12-7-12 surfactants, and a weakly exothermic, but constant enthalpy of ~1.5 to 2 kJ mol^{-1} for the 12-2-12 surfactant. It is worthy to mention again that data in Figure 3.2.1.1 B is the subtracted data, i.e. the enthalpy profile obtained for the titration of the surfactant into Aβ minus the enthalpy profile obtained for the titration of surfactant into water. This means that there is NO difference in enthalpy for the addition of surfactant to Aβ compared to the addition of surfactant to water. Such an observation does not necessarily imply no additional interaction

43

between the surfactant molecules and Aβ, but rather that the binding interactions observed are similar to those for regular micelle formation; i.e., growth of Aβ bound surfactant aggregates is likely occurring. The weak increase in particle size observed in region 2 (Figure 3.2.1.1 A) , generally, is consistent with this, particularly if one considers that growth of Aβ bound aggregates likely involves some reorganization as well, resulting in only modest changes in particle size throughout region 2. The lack of significant enthalpy change can be rationalized in terms of no significant change in hydration of the surfactant monomers in going from the micellized state (the initial state of the surfactant in the titrant syringe of the calorimeter) to the Aβ-bound state in the titration cell.

Finally, a second peak is observed in the subtracted enthalpy profiles (Region 3 in Figure 3.2.1.1 B), one that is very weakly exothermic in nature for the 12-3-12 and 12-7-12 surfactants, weakly endothermic for the 12-4-12 surfactant, and strongly endothermic for the 12-2-12 surfactant. This transition corresponds to the saturation of the Aβ peptide chains, and the onset of free micelle formation for the surfactants. In Figure 3.2.1.1 A, changes in particle size continue to be observed; however there is no clear trend observed, with both increase and decrease in particle size for all 4 surfactants. At this point added surfactant is presumed to form free micelles; however, it is important to keep in mind that there will be an on-going equilibrium between mixed gemini surfactant- Aβ aggregates, and free surfactant micelles. It should also be remembered that the aggregation of Aβ itself into pure Aβ aggregates (be they micelles, oligomers, fibrilles, etc.) is a highly time dependent process, and growth of the mixed surfactant-

Aβ aggregates may also take place. As indicated above, AFM or EM studies give us better images about the exact nature of the mixed aggregates.

Given the above discussion, it is clear that significant interaction between the gemini surfactants and Aβ do occur, and that the nature of these interactions depends on the length of the spacer group within the surfactant structure. Generally, stronger interactions appear to occur for surfactants with shorter spacer groups; however, the interpretation of the results is confounded by an apparent odd-even dependence on the number of methylene units within the spacer group (65).

3.2.2 Interactions between 12-4(OH)x-12 gemini surfactants and Aβ

In the absence of surfactant, the average particle size of Aβ peptide is ~300 nm (Figures 3.2.2.1 A). Addition of surfactant results initially in a decrease in the average particle size. At the same time the enthalpies for 12-4(OH)-12 are observed to first increase (i.e an endothermic transition) and then decrease (i.e. an exothermic transition) whereas the enthalpies for 12-4(OH)$_2$-12 initially do not change but then show an exothermic transition. As mentioned in section 3.2.1, demicellization of gemini surfactant occurs (endothermic) when concentrated surfactant is injected into the reaction cell (76); however, for 12-4(OH)$_2$-12 this endothermic demicellization may be cancelled out through increased hydrogen bonding (exothermic in nature (89)) that could occur between the head groups of 12-4(OH)$_2$-12 molecules. 12-4(OH)$_2$-12 surfactant has one extra hydroxyl group as compared to 12-4(OH)-12, and the extra hydroxyl group appears to make significant difference in the enthalpy profiles of 12-4(OH)$_2$-12.

45

The particle size data reveals decreases in particle size, which means that Aβ is dehydrated, and compacted by the added surfactant, resulting in an overall decrease in particle size, as seen in Figure 3.2.2.1 A. This interpretation could be confirmed by using AFM and EM methods in different surfactant concentrations in Aß solution.

The difference in the mono and di-substituted hydroxyl gemini surfactants enthalpy profiles can be attributed to their difference in the number of hydroxyl groups in the spacers. Therefore, OH groups in the di-substituted spacer have to occupy a gauche or eclipsed conformation, that results in enhanced steric hindrance between alkyl chains when they are in the cis or eclipsed position; that results changing in $12-4(OH)_2-12$ conformation (81,88).

Looking now at region 2, for both surfactants there is a flattening of the enthalpy profile (Figure 3.2.2.1 B) we observed that one hydroxyl group cannot be more effective than 12-s-12 surfactants in interaction with Aß. Moreover, we conclude that the effect of one additional hydroxyl group is not substantial enough to make the expected difference compare to 12-s-12 series. For $12-4(OH)_2-12$ in region 2 (Figure 3.2.2.1 B) we can see the flattening exothermic enthalpy. Also, in region 2, in DLS data (Figure 3.2.2.1 A) we see a substantial reduction in particle size. The ITC and DLS data together show that the interaction between a surfactant with two hydroxyl group in the spacer is different from 12-s-12 in Figure 3.2.1.1, region 2. It seems that the two hydroxyl groups in the spacer can be effective enough in changing Aß conformation and particle size compare to that of 12-4(OH)-12. As it is observed in Figure 3.2.2.1, region 2, significant reduction in particle size and exothermic enthalpy can be attributed to the hydrogen bonding between $12-4(OH)_2-12$ and Aß. In addition, we conclude that $12-4(OH)_2-12$ is strong

46
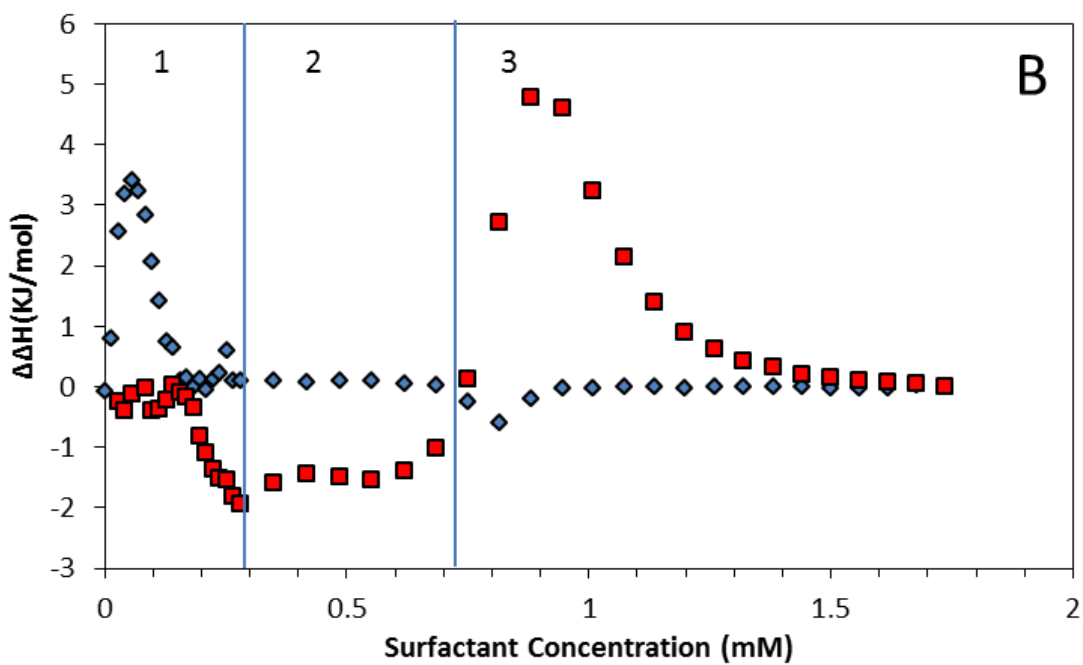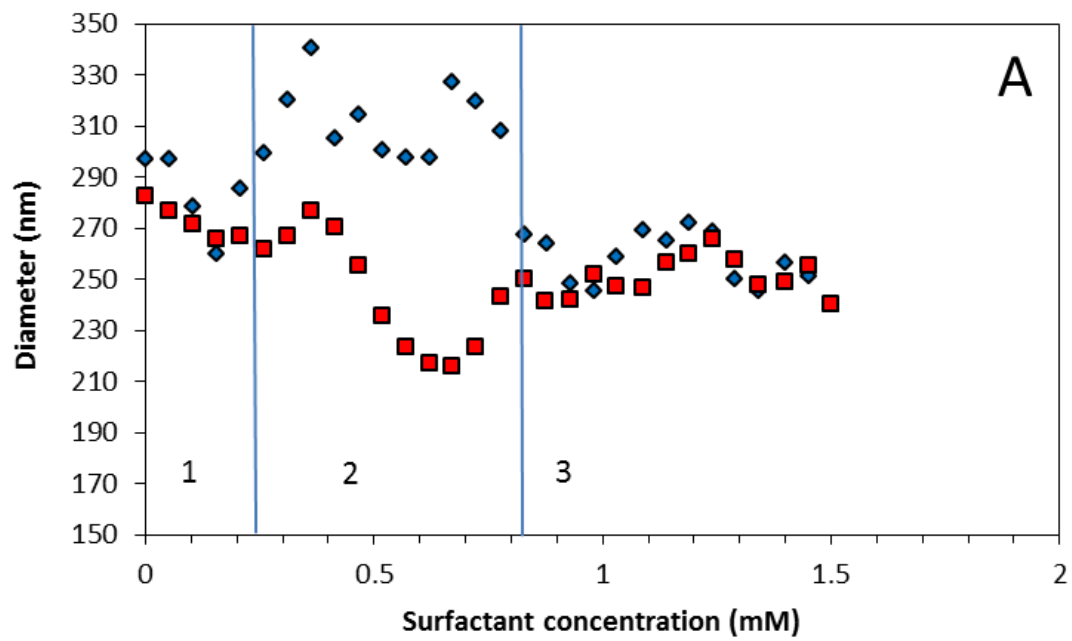
Figure 3.2.2.1. A) Dynamic light scattering and B) Observed enthalpies for the addition of 12-4(OH)-12 (◆), and 12-4(OH)$_2$-12 (■) into Aß (1μg/ml) solution.

enough to change Aß conformation: 12-4(OH)$_2$-12 attaches to Aß by hydrogen bonding. Then the addition of more surfactant molecules causes repulsion force between surfactants' head group, which leads to the dissociation of Aß aggregates (we denote this by process 1). Hence, more free spaces on Aß will be available to interact with 12-4(OH)$_2$-12. Therefore, process 1 will be repeated and the size of Aß aggregate which was produced in process 1 (now Aß aggregate has smaller size) is reduced again (Figure 3.2.2.2). Although some endothermic interactions occur which affect the exothermic interactions, all these interactions are exothermic overall.
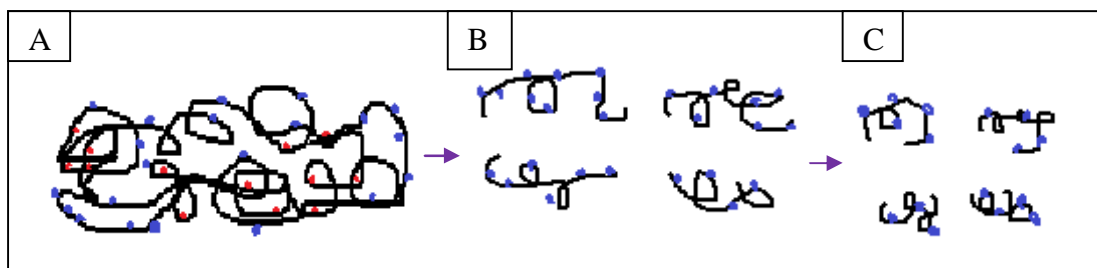
Figure 3.2.2.2. 12-4(OH)$_2$-12/Aß conformation: Aß aggregate (A), disrupted Aß (B), disrupted Aß while surfactant makes each particle smaller than part B (C). Aß (◆), Surfactant (◆), unavailable spaces with a potential to interact with gemini surfactant (◆).

Within region 3 a second peak is observed in the subtracted enthalpy profiles (Region 3 in Figure 3.2.2.1 B), and after that the enthalpies and particle sizes for both surfactants reach the point that do not change significantly (micelles consist of surfactant and Aß are forming in this region) (Figure 3.2.2.1). The peaks in Region 3 for 12-4(OH)-12 is not significant compare to that of 12-4(OH)$_2$-12, which has a significant endothermic peak in region 3. As there is no reference (to our knowledge) related to 12-4(OH)$_n$-12 interaction with polymers, the following is our own interpretation about the possible structure changes in 12-4(OH)$_2$-12 and 12-4(OH)-12

molecules in interaction with Aß. In region 3, the saturation of Aß occurs. It means that the gemini surfactant's micellar shapes are formed, which attach to Aß. The ITC data for 12-4(OH)-12 in this region shows a weak exothermic enthalpy profile. This exothermic enthalpy can be attributed to one hydroxyl group in the spacer; this hydroxyl group is in a direct contact with Aß, and based on 12-4(OH)-12 structure, there is no factor (e.g. steric hindrance) that pushes one hydroxyl group between two tail groups (inside the molecule structure). Moreover, the steric hindrance between two alkyl tails is strong enough to prevent the hydroxyl group to be placed between two alky tail groups (Figure 3.2.2.3). Therefore, the hydroxyl group position is outside of the spacer, which facilitates the interaction of gemini surfactant with Aß. In 12-4(OH)$_2$-12, we can see the endothermic peak in region 3. As we mentioned, there are two hydroxyl groups in the carbon number 2 and 3 in the spacer. In region 3, Aß is saturated with gemini surfactant molecules. Therefore, a surfactant micelle is formed and attached to Aß. As two hydroxyl groups in the spacer are close to each other, the steric hindrance prevents them to be in the same position. Hence, two hydroxyl groups will be in the gauche or eclipsed conformation (Figure 3.2.2.3B), which changes the whole molecule configuration. This configuration change affects the way that two hydroxyl groups interact with Aß. In addition, changing in the molecular configuration can be endothermic enough to cancel out the exothermic enthalpy that results from hydrogen bonding. Therefore, the different conformation of 12-4(OH)$_2$-12 in interaction with Aß causes a substantial difference in ΔH in region 3 compared to that of 12-4(OH)-12.
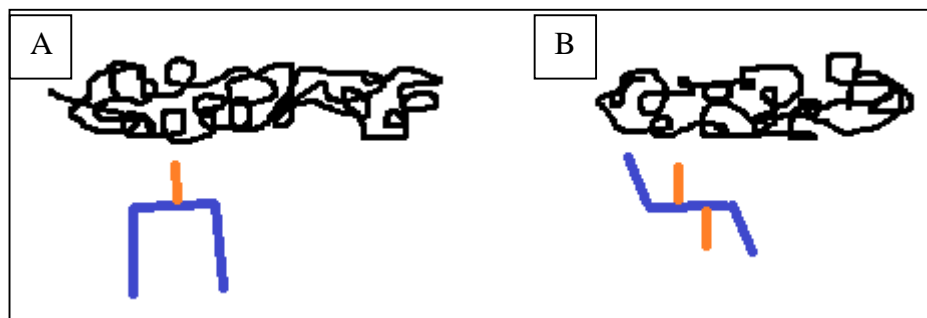
Figure 3.2.2.3. 12-4(OH)-12/Aß conformation (A), and 12-4(OH)$_2$ -12/Aß conformation (B). Aß (◆), gemini surfactant (◆), hydroxyl group (◆).

In Figure 3.2.2.1 A, we can see the changes in particle size (not significant changes). However in Figure 3.2.2.1 B, the ITC data shows flattening of enthalpy at the points close to the end of the plot. It can be concluded that the surfactant molecules attach to Aß and make micelles consisting of surfactant and Aß. These micelles are in equilibrium with the surfactant molecules in their environment.

Comparing the effect of 12-4(OH)-12 and 12-4(OH)$_2$-12 on Aß aggregates, it can be concluded that the interaction between hydroxyl-substituted gemini surfactant and Aß depends on the number of OH substitutes in the spacer. Generally, stronger interactions appear to occur for the surfactant with two OH in the spacer group as compared to the surfactant with a single OH group.

3.2.3 Interactions between 12-EOx-12 gemini surfactants and Aβ

In Figures 3.2.3.1 A and B, the particle sizes (diameter) and subtracted enthalpies (ΔH) as a function of surfactant concentration for the 12-(EO)$_x$-12 /Aβ systems are observed. As can be seen, the behavior of surfactants with different number of ethoxy groups varies due to the

different interactions that occur between surfactant and Aß. As observed in Figure 3.2.3.1 there is not a significant interaction between 12-$(EO)_1$-12 and Aß, and between 12-$(EO)_3$-12 and Aß. For 12-$(EO)_2$-12 the enthalpy profiles show significant interaction with Aß compared to those in 12-$(EO)_n$-12 series. Looking at the enthalpy profiles for all three surfactants, it is observed that 12-$(EO)_2$-12 has stronger interaction compared to the other two surfactants. As hydrophilicity of 12-$(EO)_2$-12 is more than that of 12-(EO)-12, it is expected that 12-$(EO)_2$-12/Aß interaction is stronger than 12-(EO)-12/Aß. Although 12-$(EO)_3$-12 is more hydrophilic than 12-(EO)-12 and 12-$(EO)_2$-12, yet the 12-$(EO)_3$-12/Aß interaction is not stronger than that of 12-(EO)-12/Aß and 12-$(EO)_2$-12/Aß. Using ITC and DLS techniques are not enough to help us to explain the molecular conformation changes in 12-$(EO)_3$-12 in interaction with Aß. We can propose that the conformational changes in the spacer could be responsible for decrease in 12-$(EO)_3$-12/Aß interaction.

Looking now at region 2, the enthalpies for 12-$(EO)_1$-12 and 12-$(EO)_3$-12 are approximately 0 kJ mol^{-1}. In the areas which enthalpy profiles are zero, it seems that the surfactant interaction with Aß is the same as the interaction at the end of the enthalpy plot (Figure 3.2.3.1 B) in region 3 (in region 3, the surfactant/Aß interaction causes formation of micelles consisting of Aß and surfactant).

For 12-$(EO)_2$ -12 in region 2, we see endothermic enthalpy in contrast to 12-$(EO)_1$-12 and 12-$(EO)_3$-12. We conclude that since 12-$(EO)_2$ -12 is more hydrophilic than 12-(EO)-12, and has a straight spacer (compared to the spacer of 12-$(EO)_3$-12 that, as we already proposed, it's spacer could have a different conformation rather than being straight) it can interact better with Aß than

51
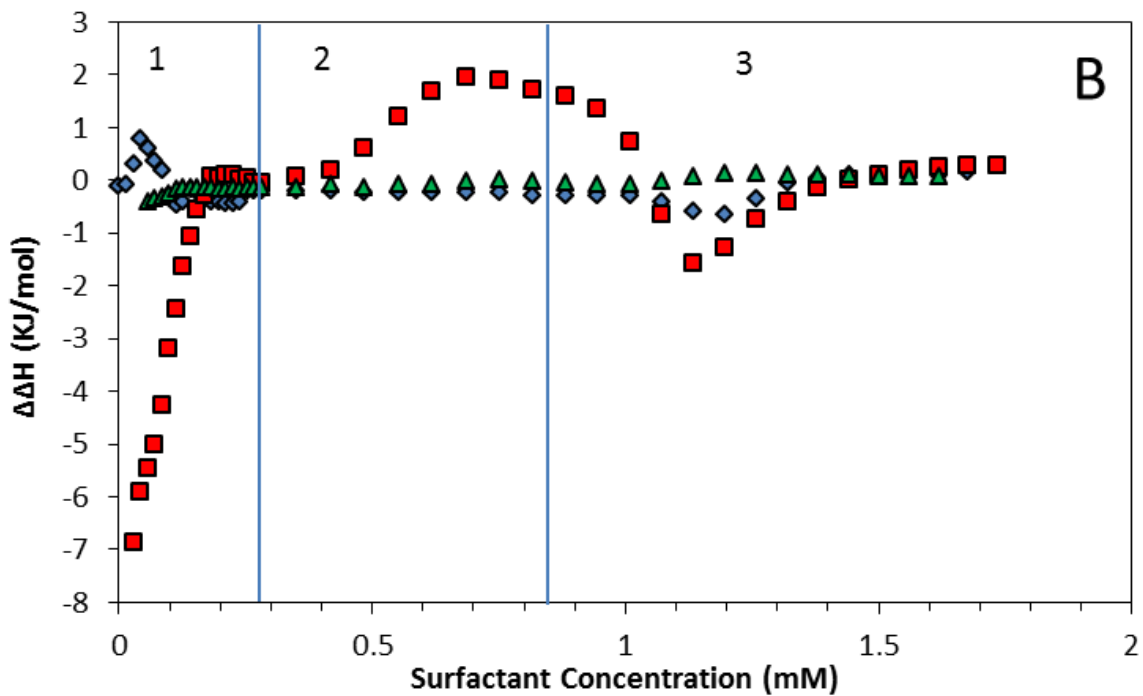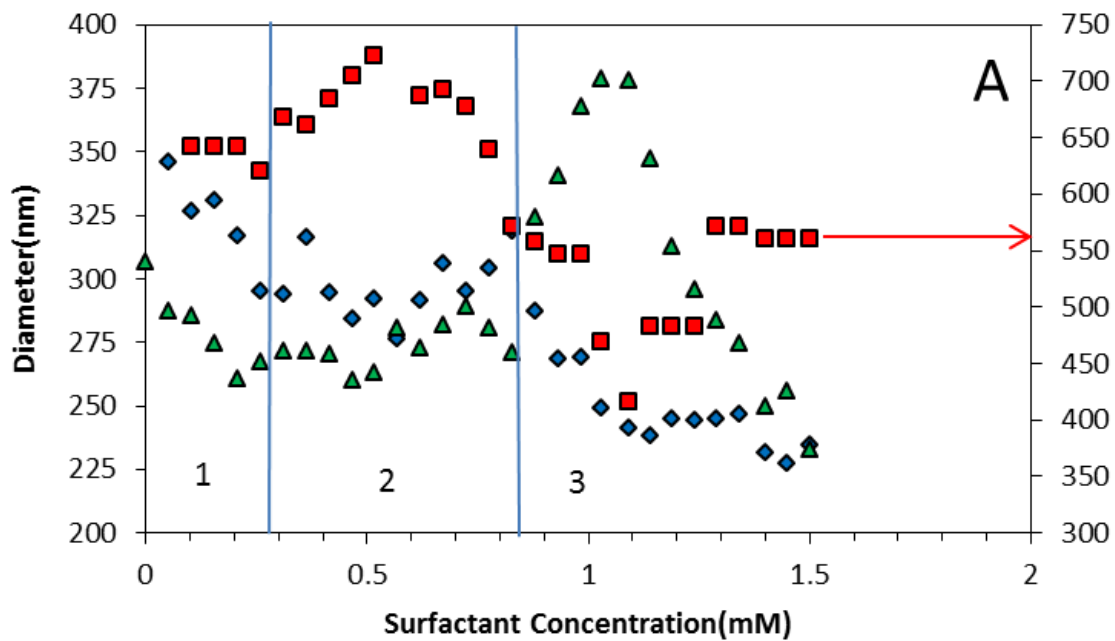
Figure 3.2.3.1. A) Dynamic light scattering and B) Observed enthalpies for the addition of 12-EO$_1$-12 (◆),12-EO$_2$-12 (■), and 12-EO$_3$-12 (▲)into Aß (1µg/ml) solution.

those with one and three ethoxy groups in the spacer. 12-(EO)$_2$ -12 can have the same interaction pattern as 12-4(OH)$_2$-12 in section 3.2.2 (Figure 3.2.2.1 B, region 2).

Finally, a second peak is observed for 12-(EO)$_2$-12 in the subtracted enthalpy profiles (Region 3 in Figure 3.2.3.1 B), for 12-(EO)-12 and 12-(EO)$_3$-12, the ITC data does not show a significant changes in enthalpy profile for both of them. As mentioned in section 3.2.1, in this region, surfactant monomers are likely to form free micelles; also the monomers can transfer from the micelles to mixed gemini surfactant-Aß aggregates since there is an equilibrium between these two structures (surfactant free micelles and surfactant-Aß aggregates). To confirm these interpretations, AFM and EM studies are needed.

Based on the above discussion the chemical groups in the spacer and the length of the spacer affect the interaction between gemini surfactant and Aß. Generally, stronger interactions are seen in 12-(EO)$_2$-12/Aß than those of 12-(EO)-12/Aß and 12-(EO)$_3$-12/ Aß.

3.2.4 Interactions between 12-XN-12 gemini surfactants and Aβ

As shown in Figure 3.2.4.1 the particle sizes (diameter) and subtracted enthalpies (ΔH) as a function of surfactant concentration for the 12-5N-12 /Aβ and 12-8N-12/Aß systems are assessed. Various behaviours in a surfactant with one aza group compared to that with two aza groups in the spacers are observed.

Before the addition of 12-5N-12 surfactant, the Aβ peptide has an average particle size of ~300 nm, and in the absence of added 12-8N-12, the Aß peptide has an average particle size of ~370. After the surfactant is added, the average particle sizes are observed to decrease for both

systems, but then an increase in particle size was observed for 12-5N-12 in region 1. At the same time the enthalpies for 12-5N-12/Aß are observed to change significantly whereas there is not substantial change in the 12-8N-12/Aß enthalpy.

In our opinion, the exothermic enthalpy in this region is attributed to the hydrophilic interaction between the spacers and Aß. Donkuru (86) et al. assessed the efficacy of aza substituted gemini surfactants in increasing transfection efficacy. They mentioned the effect of methyl groups in increasing steric hindrance between gemini surfactants and DNA molecules. We can use a similar interpretation in rationalizing the difference in the behavior of 12-5N-12/Aß and 12-8N-12/Aß. As it is shown in Figure 3.2.4.2, the methyl group in 12-5N-12 is not as effective as two methyl groups in 12-8N-12 in reducing the surfactant interactions with Aß. Hence, the significantly higher exothermic transition of 12-5N-12/Aß in region 1 compared to that of 12-8N-12/Aß (Figure 3.2.4.1 B) can be explained by the higher hydrophilic interaction between 12-5N-12 and Aß versus that between 12-8N-12 and Aß.

The particle size data in region 1 (Figure 3.2.4.1 A) shows first a slight decrease and then significant increase in 12-5N-12/Aß particle size. 12-5N-12 molecules tend to attach to Aß and unfold the Aß aggregates. This creates availability for more parts of the Aß aggregate to accept 12-5N-12 molecules (Figure 3.2.4.3). Hence, unfolded Aß can bind more surfactant molecules and this process is responsible for an increased particle size in region 1 for 12-5N-12. AFM or EM methods can give us better images of gemini surfactant/Aß interaction, which would help us to confirm our interpretation of their interaction.

54
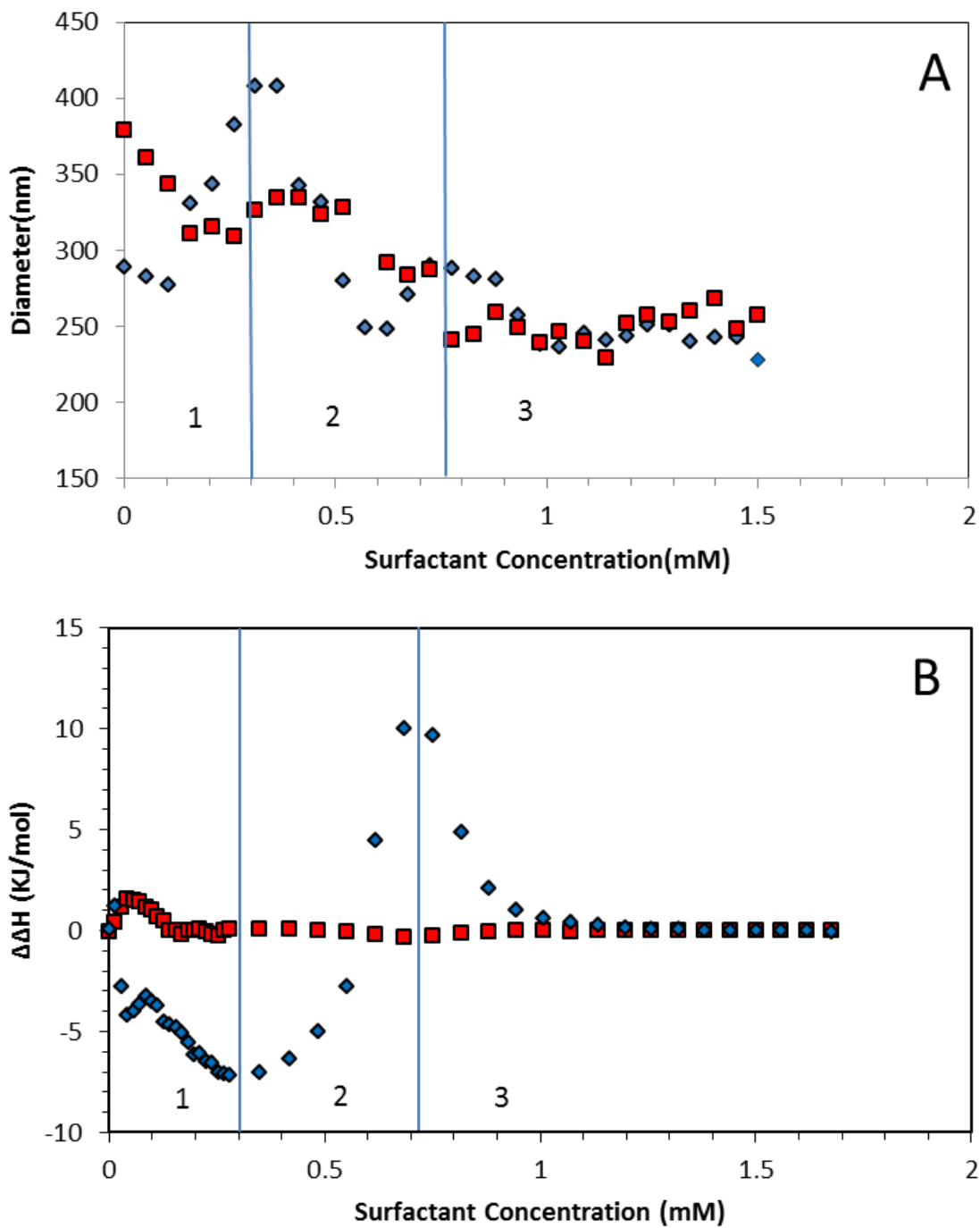
Figure 3.2.4.1. A) Dynamic light scattering and B) Observed enthalpies for the addition of 12-5N-12 (◆), and 12-8N-12 (■) into Aß (1μg/ml) solution.
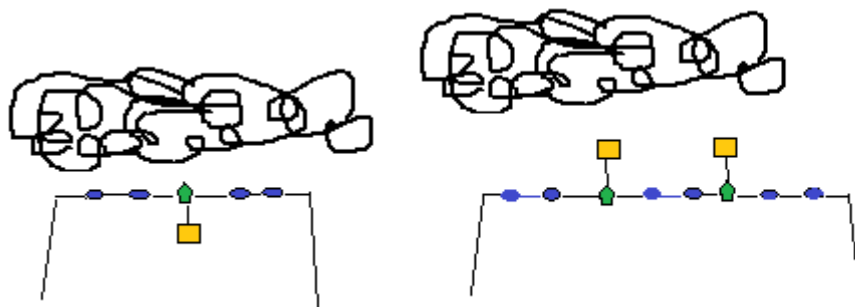
Figure 3.2.4.2. 12-5N-12/Aß conformation (A), 12-8N-12/Aß conformation (B): Aß (◆),Carbon (●), Nitrogen (⬟), Methyl group (▢).

Looking now at region 2, for 12-5N-12 there is an endothermic enthalpy profile (an endothermic transition) (Figure 3.2.4.1 B), and for 12-8N-12 the enthalpy profiles being approximately zero, and weakly exothermic. The flattening enthalpy reveals that there is no difference in enthalpy for the addition of surfactant to Aβ compared to the addition of surfactant to water. Thus, one can assume that 12-8N-12 molecules are added to Aß in this region are forming micelles. The increase in particle size observed in region 2 (Figure 3.2.4.1 A), is consistent with the above interpretation, and also the fact that reorganization of Aß could occur in this region that results in the increasing in particle size.

In 12-5N-12, interactions with Aß are different in region 2 from 12-8N-12/Aß interactions. In region 2 in DLS data (3.2.4.1 B) after the increasing of particle size, we see a significant reduction in particle size for 12-5N-12. The enthalpy change for 12-5N-12 is significant in this region, which can be related to the high endothermic interactions between surfactant and Aß. Based on DLS and ITC data in region 2, we conclude that the attachment of

12-5N-12 to Aß causes unfolding of the aggregate. The difference in the enthalpy profiles for 12-5N-12 and 12-8N-12 in region 2 is attributed to an extra aza group in 12-8N-12, which previously discussed in this section that how one extra methyl group in the spacer could affect the interaction between aza substituted surfactant and Aß.

Region 3 corresponds to the saturation of Aβ peptide, and the onset of free micelle formation for the surfactants. In Figure 3.2.4.1 A, a change in particle size is observed. At this point, added surfactant forms free micelles. There is also equilibrium between mixed gemini surfactant- Aβ aggregates and free surfactant micelles.

Based on above discussion, it can be concluded that the number of aza groups in the spacer has a significant impact on surfactant/Aß interaction. Generally, stronger interactions appear to occur for 12-5N-12; although two aza groups seems to have more hydrophilic interaction with Aß than that of 12-5N-12, the steric hindrance caused by two methyl groups in the spacer reduces the interaction of 12-8N-12 and Aß.

3.2.5 Summary of ITC and DLS results

To our knowledge, none of the articles about gemini surfactant/Aß interactions (for example (50,72,76,77,90)) mentioned a detailed or properly supported explanation about the interaction between gemini surfactant and Aß. In this work, we have the data for different surfactants with different spacer structures. This gives us a substantial amount of data, compared to most of the papers in the literature, and helps us to present stronger interpretations by comparison between the data of different surfactants.

Among eleven surfactants, the strongest interactions are seen in 12-$(EO)_2$-12/Aß, 12-4$(OH)_2$-12/Aß and 12-5N-12/Aß systems. To confirm our work, other techniques such as NMR, AFM and dialysis-based binding studies can be used.

Chapter 4: Conclusions

Within this work, the physicochemical properties of the interaction between gemini surfactants with different spacer groups and Aß peptide were assessed. First, we evaluated the interactions by surface tension measurements. We observed changes in cmc and head group area of our gemini surfactants in Aß solution. It was obvious that gemini surfactants with different spacer length and various spacer substitutes can interact with Aß, and we conclude this interaction is through a solubilization process, rather than a more typical surfactant/polymer or surfactant/protein interaction as introduced in Chapter 1. Our surface tension results do not show the cac and C_2 critical concentrations expected for surfactant/polymer systems and instead clearly show a reduction in cmc for most surfactants, as expected for micelle formation in the presence of a hydrophobic solute. From variations in the head group areas for the surfactants it is also clear that there is substantial interaction occurring between the surfactants and Aß; however the nature of this interaction (i.e. arrangement of surfactant and peptide within each aggregate) remains unclear.

As the surface tension data did not give us enough information about the gemini surfactant/Aß interaction, we decided to use ITC and dynamic light scattering techniques to confirm our results in surface tension part and also get a better idea about the possible interactions occurring between gemini surfactant and Aß. The ITC results reveal that gemini surfactant with different spacer groups do not follow the same trend in interaction with Aß. For example, it was observed that gemini surfactant with hydroxyl group in the spacer interacts with Aß differently from those with ethoxy or aza groups. The hydrogen bond between $12\text{-}4(OH)_n\text{-}12$

and Aß is a factor that affects the whole molecule interaction with Aß. In 12-(EO)$_n$ -12 gemini surfactants, there is still hydrophilic interaction that can affect whole molecule configuration. In gemini surfactants with aza groups in their spacer the hydrophilicity of the spacer plays an important role in 12-XN-12 interaction with Aß. The DLS experiments help us to get better idea about the particle size changes in different gemini surfactant concentration in interaction with Aß. Overall, it was observed that the particle size decrease at the end of the experiment. These results reveal that gemini surfactant molecules with various spacers are able to disrupt Aß aggregates and turn them into smaller particles.

Future directions of research

Aß plays an important role in the pathophysiology of Alzheimer's disease. In this research we tried to investigate the effect of gemini surfactants' spacer on Aß aggregation and formation. AFM studies can be helpful in confirming what we proposed in our research about the Aß/gemini surfactant configuration. It can reveal the spacer's structure effects on the overall configuration of gemini surfactant/Aß interaction. Aggregation assay is another experiment that can be helpful in checking the aggregation status of Aß before and after adding gemini surfactant. Testing the neuronal cell toxicity of gemini surfactant and also gemini surfactant's efficacy in reducing Aß toxicity for neuronal cells is another experiment that can be conducted. The MTT assay is the experiment that can be used in testing the neuronal cell toxicity of molecules.

Appendix 1
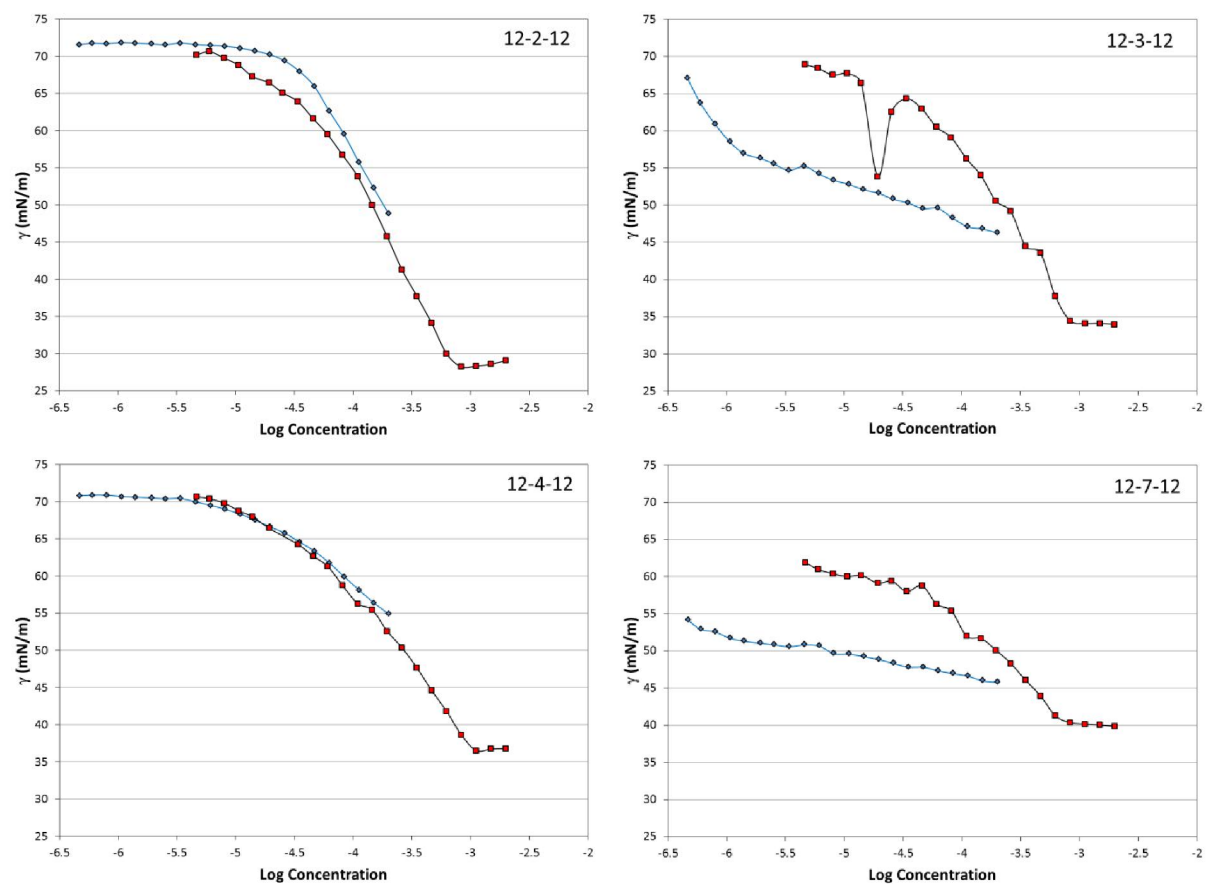
Figure A.1.1: Surface tension plot for the titration of the 12-s-12 gemini surfactants (◆ = 1 mM stock solution; ■ = 10 mM stock solution) into a 1 µg/mL solution of Aβ in water.
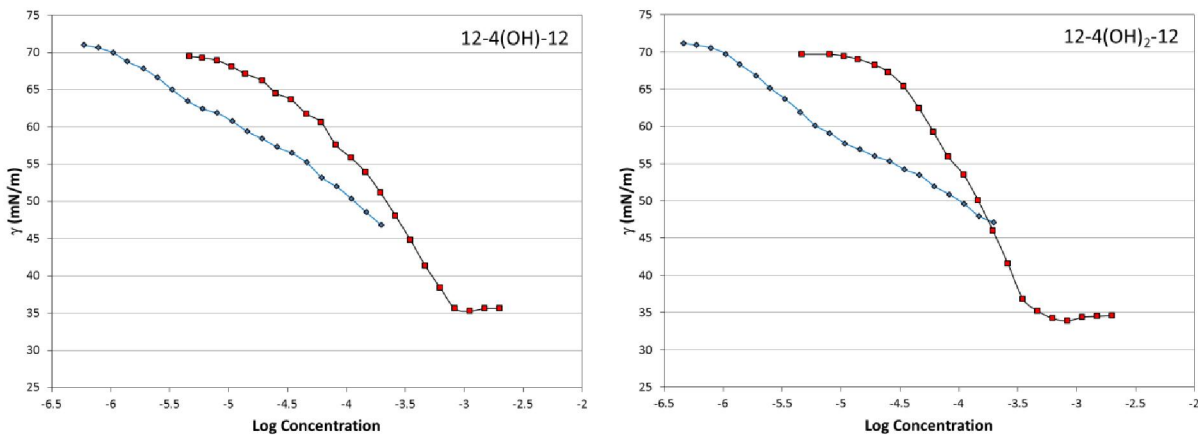
Figure A1.2: Surface tension plot for the titration of the 12-4(OH)$_x$-12 gemini surfactants ($\blacklozenge$ = 1 mM stock solution; $\blacksquare$ = 10 mM stock solution) into a 1 μg/mL solution of Aβ in water.
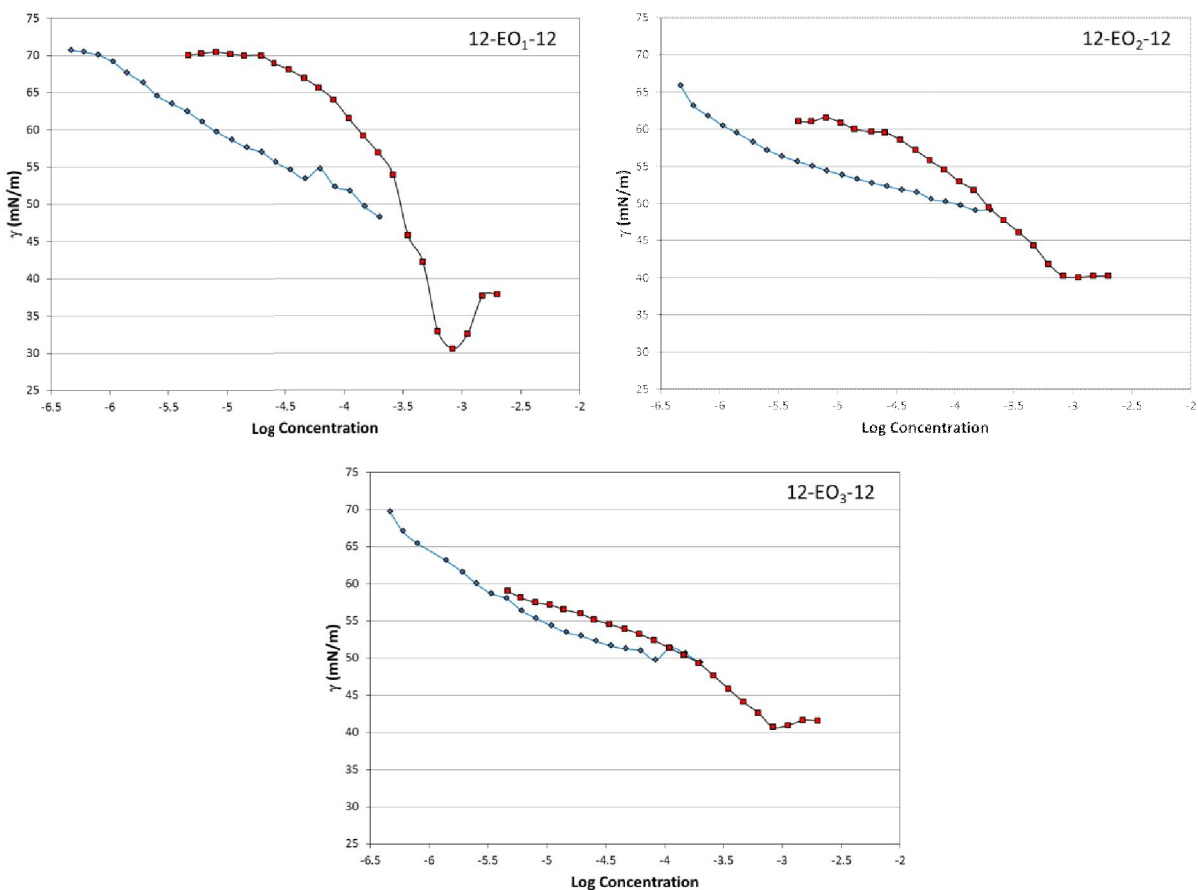
Figure A1.3: Surface tension plot for the titration of the 12-EO$_x$-12 gemini surfactants ($\blacklozenge$ = 1 mM stock solution; $\blacksquare$ = 10 mM stock solution) into a 1 μg/mL solution of Aβ in water.
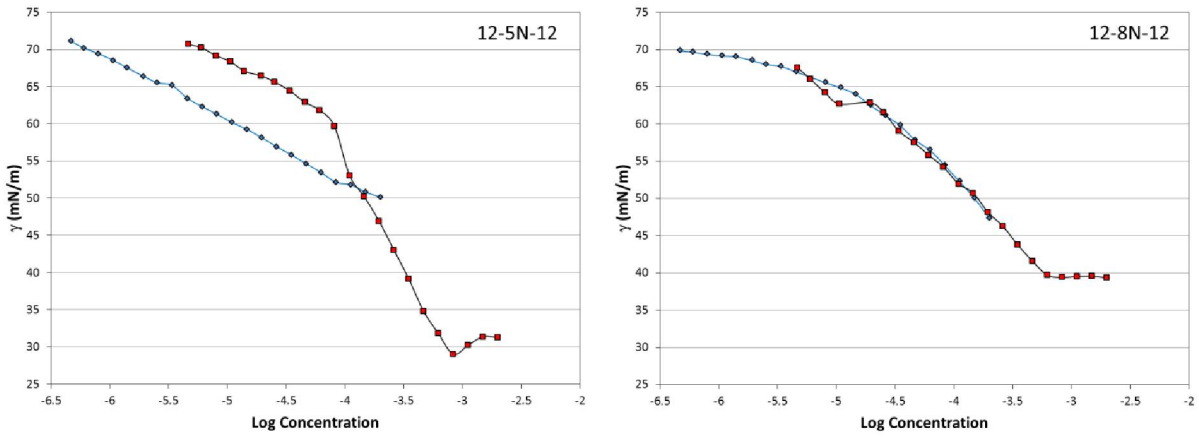
Figure A1.4: Surface tension plot for the titration of the 12-XN-12 gemini surfactants (◆ = 1 mM stock solution; ■ = 10 mM stock solution) into a 1 µg/mL solution of Aβ in water.

References

(1) Pillai JA, Cummings JL. Clinical Trials in Predementia Stages of Alzheimer Disease. Med Clin North Am 2013 5;97(3):439-457.

(2) Stopford CL, Snowden JS, Thompson JC, Neary D. Distinct Memory Profiles in Alzheimer's Disease. Cortex 2007;43(7):846-857.

(3) Lopez OL, Schwam E, Cummings J, Gauthier S, Jones R, Wilkinson D, et al. Predicting cognitive decline in Alzheimer's disease: An integrated analysis. Alzheimer's & Dementia 2010 11;6(6):431-439.

(4) Lyketsos CG, Carrillo MC, Ryan JM, Khachaturian AS, Trzepacz P, Amatniek J, et al. Neuropsychiatric symptoms in Alzheimer's disease. Alzheimer's & Dementia 2011 9;7(5):532-539.

(5) Marshall GA, Rentz DM, Frey MT, Locascio JJ, Johnson KA, Sperling RA. Executive function and instrumental activities of daily living in mild cognitive impairment and Alzheimer's disease. Alzheimer's & Dementia 2011 5;7(3):300-308.

(6) Marshall GA, Fairbanks LA, Tekin S, Vinters HV, Cummings JL. Neuropathologic correlates of activities of daily living in Alzheimer disease. Alzheimer Dis Assoc Disord 2006;20(1):56-59.

(7) Alistair Burns, Steve Iliffe. Alzheimer's disease. BMJ 2009 BMJ Publishing Group Ltd;338.

(8) Nadkarni NK, Levy-Cooperman N, Black SE. Functional correlates of instrumental activities of daily living in mild Alzheimer's disease. Neurobiol Aging 2012 1;33(1):53-60.

(9) Ferri C, Sousa R, Albanese E, Ribeiro W, Honyashiki M, . World alzheimer report. 2009; Available at: http://www.alz.co.uk/research/files/WorldAlzheimerReport.pdf.

(10) Bartus RT, Dean RL, Beer B, Lippa AS. The Cholinergic Hypothesis of Geriatric Memory Dysfunction. Science 1982 Jul. 30;217(4558):408-417.

(11) van Marum RJ. Current and future therapy in Alzheimer's disease. Fundam Clin Pharmacol 2008;22(3):265-274.

(12) Bartus RT. Evidence for a direct cholinergic involvement in the scopolamine-induced amnesia in monkeys: Effects of concurrent administration of physostigmine and methylphenidate with scopolamine. Pharmacology, Biochemistry and Behavior 1978 Dec;9(6):833-836.

(13) Craig LA, Hong NS, McDonald RJ. Revisiting the cholinergic hypothesis in the development of Alzheimer's disease. Neuroscience & Biobehavioral Reviews 2011 5;35(6):1397-1409.

(14) Xu Y, Yan J, Zhou P, Li J, Gao H, Xia Y, et al. Neurotransmitter receptors and cognitive dysfunction in Alzheimer's disease and Parkinson's disease. Prog Neurobiol 2012 4;97(1):1-13.

(15) Barrantes FJ, Borroni V, Vallés S. Neuronal nicotinic acetylcholine receptor–cholesterol crosstalk in Alzheimer's disease. FEBS Lett 2010 May 03;584(9):1856-1863.

(16) Medeiros R, Kitazawa M, Caccamo A, Baglietto-Vargas D, Estrada-Hernandez T, Cribbs DH, et al. Loss of Muscarinic M1 Receptor Exacerbates Alzheimer's Disease–Like Pathology and Cognitive Decline. The American Journal of Pathology 2011 201108;179(2):980-991.

(17) Turner TJ. Nicotine Enhancement of Dopamine Release by a Calcium-Dependent Increase in the Size of the Readily Releasable Pool of Synaptic Vesicles. The Journal of Neuroscience 2004 December 15;24(50):11328-11336.

(18) Castellani RJ, Rolston RK, Smith MA. Alzheimer Disease. Disease-a-Month 2010 Sept;56(9):484-546.

(19) Giacobini E. Do Cholinesterase Inhibitors Have Disease-Modifying Effects in Alzheimer's Disease? CNS Drugs 2001 Feb;15(2):85-91.

(20) Whitehouse P. Quality of life: The bridge from the cholinergic basal forebrain to cognitive science and bioethics. J Alzheimers Dis 2006;9(3):447-553.

(21) Hebert LE, Scherr PA, Bienias JL, Bennett DA, Evans DA. Alzheimer disease in the US population: prevalence estimates using the 2000 census. Archives of Neurology 2003 August;60(8):1119-1122.

(22) Tolnay , Probst . REVIEW: tau protein pathology in Alzheimer's disease and related disorders. Neuropathol Appl Neurobiol 1999;25(3):171-187.

(23) Alonso AC, Zaidi T, Grundke-Iqbal I, Iqbal K. Role of abnormally phosphorylated tau in the breakdown of microtubules in Alzheimer disease. Proceedings of the National Academy of Sciences 1994 June 07;91(12):5562-5566.

(24) Weingarten MD, Lockwood AH, Hwo SY, Kirschner MW. A protein factor essential for microtubule assembly. Proceedings of the National Academy of Sciences 1975 May;72(5):1858-1862.

(25) Iqbal K, del C. Alonso A, Chen S, Chohan MO, El-Akkad E, Gong CX, et al. Tau pathology in Alzheimer disease and other tauopathies. BBA - Molecular Basis of Disease 2005;1739(2-3):198-210.

(26) Luan K, Rosales JL, Lee K. Viewpoint: Crosstalks between neurofibrillary tangles and amyloid plaque formation. Ageing Research Reviews 2013 1;12(1):174-181.

(27) Martin L, Latypova X, Wilson CM, Magnaudeix A, Perrin M, Terro F. Tau protein phosphatases in Alzheimer's disease: The leading role of PP2A. Ageing Research Reviews 2013 1;12(1):39-49.

(28) Avila J. Tau phosphorylation and aggregation in Alzheimer's disease pathology. FEBS Lett 2006;580(12):2922-2927.

(29) Trojanowski JQ, Lee VM. Phosphorylation of paired helical filament tau in Alzheimer's disease neurofibrillary lesions: focusing on phosphatases. The FASEB Journal 1995 Dec;9(15):1570-1576.

(30) Querfurth HW, LaFerla FM. Alzheimer's Disease. N Engl J Med 2010 Jan;362(4):329-344.

(31) Serpell LC. Alzheimer's amyloid fibrils: structure and assembly. Biochimica et Biophysica Acta (BBA)/Molecular Basis of Disease 2000;1502(1):16-30.

(32) Müller T, Meyer HE, Egensperger R, Marcus K. The amyloid precursor protein intracellular domain (AICD) as modulator of gene expression, apoptosis, and cytoskeletal dynamics—Relevance for Alzheimer's disease. Prog Neurobiol 2008 8;85(4):393-406.

(33) Yang M, Teplow DB. Amyloid β-Protein Monomer Folding: Free-Energy Surfaces Reveal Alloform-Specific Differences. J Mol Biol 2008 Dec;384(2):450-464.

(34) Yates D, McLoughlin DM. The molecular pathology of Alzheimer's disease. Psychiatry 2008 1;7(1):1-5.

(35) DaSilva KA, Shaw JE, McLaurin J. Amyloid-β fibrillogenesis: Structural insight and therapeutic intervention. Exp Neurol 2010 6;223(2):311-321.

(36) Sabaté R, Estelrich J. Evidence of the Existence of Micelles in the Fibrillogenesis of ß-Amyloid Peptide. The Journal of Physical Chemistry B 2005;109(21):11027-11032.

(37) Hardy JA, Higgins GA. Alzheimer's Disease: The Amyloid Cascade Hypothesis. Science 1992 Apr. 10;256(5054):184-185.

(38) Sastre M, Dewachter I, Rossner S, Bogdanovic N, Rosen E, Borghgraef P, et al. Nonsteroidal anti-inflammatory drugs repress β-secretase gene promoter activity by the activation of PPARγ. Proceedings of the National Academy of Sciences of the United States of America 2006 January 10;103(2):443-448.

(39) Siemers ER, Quinn JF, Kaye J, Farlow MR, Porsteinsson A, Tariot P, et al. Effects of a gamma-secretase inhibitor in a randomized study of patients with Alzheimer disease. Neurology 2006 Feb 28;66(4):602-604.

(40) Gilman S, Koller M, Black RS, Jenkins L, Griffith SG, Fox NC, et al. Clinical effects of Abeta immunization (AN1792) in patients with AD in an interrupted trial. Neurology 2005 May 10;64(9):1553-1562.

(41) Orgogozo JM, Gilman S, Dartigues JF, Laurent B, Puel M, Kirby LC, et al. Subacute meningoencephalitis in a subset of patients with AD after Abeta42 immunization. Neurology 2003 Jul 8;61(1):46-54.

(42) Winblad B, Andreasen N, Minthon L, Floesser A, Imbert G, Dumortier T, et al. Safety, tolerability, and antibody response of active Abeta immunotherapy with CAD106 in patients with Alzheimer's disease: randomised, double-blind, placebo-controlled, first-in-human study. Lancet Neurol 2012 Jul;11(7):597-604.

(43) Farlow M, Arnold SE, van Dyck CH, Aisen PS, Snider BJ, Porsteinsson AP, et al. Safety and biomarker effects of solanezumab in patients with Alzheimer's disease. Alzheimers Dement 2012 Jul;8(4):261-271.

(44) Salloway S, Sperling R, Gilman S, Fox NC, Blennow K, Raskind M, et al. A phase 2 multiple ascending dose trial of bapineuzumab in mild to moderate Alzheimer disease. Neurology 2009 Dec 15;73(24):2061-2070.

(45) Solomon B, Frenkel D. Immunotherapy for Alzheimer's disease. Neuropharmacology 2010 Sept;59(4–5):303-309.

(46) Barbour R, Bard F, Burke R, Cannon C, Games D, Grajeda H, et al. Peripherally administered antibodies against amyloid beta]-peptide enter the central nervous system and reduce pathology in a mouse model of Alzheimer disease. Nat Med 2000 Aug;6(8):916-919.

(47) DeMattos RB, Bales KR, Cummins DJ, Paul SM, Holtzman DM. Brain to plasma amyloid-beta efflux: a measure of brain amyloid burden in a mouse model of Alzheimer's disease. Science 2002 Mar 22;295(5563):2264-2267.

(48) Barnes K, Turner AJ. The endothelin system and endothelin-converting enzyme in the brain: molecular and cellular studies. Neurochem Res 1997 Aug;22(8):1033-1040.

(49) Nalivaeva NN, Beckett C, Belyaev ND, Turner AJ. Are amyloid-degrading enzymes viable therapeutic targets in Alzheimer's disease? J Neurochem 2012 Jan;120 Suppl 1:167-185.

(50) Han Y, Wang Y. Aggregation behavior of gemini surfactants and their interaction with macromolecules in aqueous solution. Phys Chem Chem Phys 2011;13(6):1939-1956.

(51) Sabaté R, Estelrich J. Stimulatory and Inhibitory Effects of Alkyl Bromide Surfactants on β-Amyloid Fibrillogenesis. Langmuir 2005;21(15):6944-6949.

(52) - He C, Hou Y, Han Y, Wang Y. Disassembly of Amyloid Fibrils by Premicellar and Micellar Aggregates of a Tetrameric Cationic Surfactant in Aqueous Solution. Langmuir 2011;27(8):4551-4556.

(53) - Bao H, Li L, Huat Gan L, and Zhang H. Interactions between Ionic Surfactants and Polysaccharides in Aqueous Solutions. Macromolecules 2008; 41(23):9406-9412.

(54) Li Y, Xu R, Couderc S, Bloor DM, Holzwarth JF, Wyn-Jones E. Binding of Tetradecyltrimethylammonium Bromide to the ABA Block Copolymer Pluronic F127 (EO97 PO69 EO97): Electromotive Force, Microcalorimetry, and Light Scattering Studies. Langmuir 2001;17(19):5742-5747.

(55) Shirahama K. The nature of polymer-surfactant interactions. In: Kwak, editor. Polymer-surfactant systems. New York: M. Dekker; 1998. p.143-191.

(56) Myers D. Surfactant science and technology. Hoboken: John Wiley & Sons; 2006.

(57) Tam KC, Wyn-Jones E. Insights on polymer surfactant complex structures during the binding of surfactants to polymers as measured by equilibrium and structural techniques. Chem Soc Rev 2006;35(8):693-709.

(58) Surfactants and polymers in aqueous solution. Chichester, West Sussex, England ; Hoboken, NJ: John Wiley & Sons; 2003.

(59) Surfactants and polymers in aqueous solution. Chichester, West Sussex, England ; Hoboken, NJ: John Wiley & Sons; 2003.

(60) Otzen D. Protein–surfactant interactions: A tale of many states. Biochimica et Biophysica Acta (BBA) - Proteins & Proteomics 2011 5;1814(5):562-591.

(61) Bouchemal K. New challenges for pharmaceutical formulations and drug delivery systems characterization using isothermal titration calorimetry. Drug Discov Today 2008 Nov;13(21-22):960-972.

(62) Zana R, Xia J. Introduction. In: Zana R, Xia J, editors. Gemini surfactants : synthesis, interfacial and solution-phase behavior, and applications. New York ; Basel: Marcel Dekker; 2004. p.1-8.

(63) Javed Raymond Akbar. Pharmaceutical applications of gemini surfactants. Waterloo, Ont.: University of Waterloo; 2010.

(64) zana 2 Gemini surfactants : synthesis, interfacial and solution-phase behavior, and applications. New York ; Basel: New York ; Basel : Marcel Dekker; 2004.

(65) Li Y, Li P, Wang J, Wang Y, Yan H, Thomas RK. Odd/Even Effect in the Chain Length on the Enthalpy of Micellization of Gemini Surfactants in Aqueous Solution. Langmuir 2005;21(15):6703-6706.

(66) Wang H, Wettig SD. Synthesis and aggregation properties of dissymmetric phytanyl-gemini surfactants for use as improved DNA transfection vectors. Phys Chem Chem Phys 2010;13(2):637-642.

(67) Wang C, Li X, Wettig SD, Badea I, Foldvari M, Verrall RE. Investigation of complexes formed by interaction of cationic gemini surfactants with deoxyribonucleic acid. Phys Chem Chem Phys 2007;9(13):1616-1628.

(68) Wang C, Wettig SD, Foldvari M, Verrall RE. Synthesis, Characterization, and Use of Asymmetric Pyrenyl-Gemini Surfactants as Emissive Components in DNA-Lipoplex Systems. Langmuir 2007;23(17):8995-9001.

(69) Foldvari M, Badea I, Wettig S, Verrall R, Bagonluri M. Structural characterization of novel gemini non-viral DNA delivery systems for cutaneous gene therapy. Journal of Experimental Nanoscience 2006 June 2006;1(2):165-176.

(70) Rocha S, Loureiro JA, Brezesinski G, Pereira MdC. Peptide–surfactant interactions: Consequences for the amyloid-beta structure. Biochem Biophys Res Commun 2012 Mar;420(1):136-140.

(71) Friedman R, Caflisch A. Surfactant Effects on Amyloid Aggregation Kinetics. J Mol Biol 2011 Nov;414(2):303-312.

(72) Han Y, He C, Cao M, Huang X, Wang Y, Li Z. Facile Disassembly of Amyloid Fibrils Using Gemini Surfactant Micelles. Langmuir 2010;26(3):1583-1587.

(73) Pertinhez TA, Bouchard M, Smith RAG, Dobson CM, Smith LJ. Stimulation and inhibition of fibril formation by a peptide in the presence of different concentrations of SDS. FEBS Lett 2002;529(2-3):193-197.

(74) Shao H, Jao S, Ma K, Zagorski MG. Solution structures of micelle-bound amyloid β-(1-40) and β-(1-42) peptides of Alzheimer's disease. J Mol Biol 1999 Jan;285(2):755-773.

(75) Wood SJ, MacKenzie L, Maleeff B, Hurle MR, Wetzel R. Selective Inhibition of A Fibril Formation. Journal of Biological Chemistry 1996 February 23;271(8):4086-4092.

(76) Li Y, Cao M, Wang Y. Alzheimer Amyloid β(1−40) Peptide: Interactions with Cationic Gemini and Single-Chain Surfactants. J Phys Chem B 2006;110(36):18040-18045.

(77) Cao M, Han Y, Wang J, Wang Y. Modulation of Fibrillogenesis of Amyloid â(1-40) Peptide with Cationic Gemini Surfactant. Journal of Physical Chemistry B 2007;111:13436-13443.

(78) - Zana R, Benrraou M, Rueff R. Alkanediyl-.alpha.,.omega.-bis(dimethylalkylammonium bromide) surfactants. 1. Effect of the spacer chain length on the critical micelle concentration and micelle ionization degree. Langmuir 1991;7(6): 1072–1075.

(79) Yang P, Singh J, Wettig S, Foldvari M, Verrall RE, Badea I. Enhanced gene expression in epithelial cells transfected with amino acid-substituted gemini nanoparticles. European Journal of Pharmaceutics and Biopharmaceutics 2010 Aug;75(3):311-320.

(80) Wettig SD, Li X, Verrall RE. Thermodynamic and Aggregation Properties of Gemini Surfactants with Ethoxylated Spacers in Aqueous Solution. Langmuir 2003;19(9):3666-3670.

(81) Wettig SD, Nowak P, Verrall RE. Thermodynamic and Aggregation Properties of Gemini Surfactants with Hydroxyl Substituted Spacers in Aqueous Solution. Langmuir 2002;18(14):5354-5359.

(82) Wettig SD, Verrall RE. Thermodynamic Studies of Aqueous m–s–m Gemini Surfactant Systems. J Colloid Interface Sci 2001;235(2):310-316.

(83) Wettig SD, Wang C, Verrall RE, Foldvari M. Thermodynamic and aggregation properties of aza- and imino-substituted gemini surfactants designed for gene delivery. Phys Chem Chem Phys 2007;9(7):871-877.

(84) Kaur T, Tavakoli N, Slavcev R, Wettig S. Isothermal titration calorimetry. In: Piraján J, editor. Thermodynamics - Kinetics of dynamic systems. Coratia: InTech; 2011. p. 255-276.

 (83) Pierce MM, Raman CS, Nall BT. Isothermal Titration Calorimetry of Protein–Protein Interactions. Methods 1999;19(2):213-221. (85) Pierce MM, Raman CS, Nall BT. Isothermal Titration Calorimetry of Protein–Protein Interactions. Methods 1999;19(2):213-221.

(86) Donkuru M. Non-viral gene delivery with pH-sensitive gemini nanoparticles: synthesis of gemini surfactant building blocks, characterization and in vitro screening of transfection efficiency and toxicity Master's. [dissertation on the Internet]. [Saskatoon]: College of Pharmacy and Nutrition, University of Saskatchewan; 2008 [cited 2013 June 25]. Available from: http://ecommons.usask.ca/bitstream/handle/10388/etd-01132009-131423/mcdthesis.pdf

(87) Lindman B, Thalberg K. In: Interactions of Surfactants with Polymers and Proteins, Goddard E, Amanthapadmanabhan K.P. editors, CRC Press Inc. Boca Raton, Fl. 1993

(88) Grosmaire L, Chorro M, Chorro C, Partyka S, Zana R. Alkanediyl-α,ω-Bis(dimethylalkylammonium Bromide) Surfactants. Journal of Colloid and Interface Science 2002;246(1):175-181.

(89) Jeffrey GA, 1915-, Jeffrey GA, 1915-. An introduction to hydrogen bonding. New York ; Oxford: New York ; Oxford : Oxford University Press; 1997.

(90) He C, Hou Y, Han Y, Wang Y. Disassembly of Amyloid Fibrils by Premicellar and Micellar Aggregates of a Tetrameric Cationic Surfactant in Aqueous Solution. Langmuir 2011;27(8):4551-4556.